Apis mellifera venom induces different cell death pathways in *Trypanosoma cruzi*

CAMILA M. ADADE, GABRIELA S. F. CHAGAS *and* THAÏS SOUTO-PADRÓN*

Laboratório de Biologia Celular e Ultraestrutura, Departamento de Microbiologia Geral, Instituto de Microbiologia Paulo de Góes, Centro de Ciências da Saúde, bloco I and Instituto Nacional de Ciência e Tecnologia em Biologia Estrutural e Bioimagens, Universidade Federal do Rio de Janeiro, Ilha do Fundão, Rio de Janeiro, RJ 21941-590, Brazil

(*Received 25 January 2012; revised 21 March 2012; accepted 13 April 2012; first published online 19 July 2012*)

SUMMARY

Chagas disease chemotherapy is based on drugs that exhibit toxic effects and have limited efficacy, such as Benznidazole. Therefore, research into new chemotherapeutic agents from natural sources needs to be exploited. *Apis mellifera* venom consists of many biologically active molecules and has been reported to exhibit remarkable anti-cancer effects, often promoting an apoptosis-like death phenotype. This study demonstrates that *A. mellifera* venom can affect the growth, viability and ultrastructure of all *Trypanosoma cruzi* developmental forms, including intracellular amastigotes, at concentrations 15- to 100-fold lower than those required to cause toxic effects in mammalian cells. The ultrastructural changes induced by the venom in the different developmental forms led us to hypothesize the occurrence of different programmed cell death pathways. Autophagic cell death, characterized by the presence of autophagosomes-like organelles and a strong monodansyl cadaverine labelling, appears to be the main death mechanism in epimastigotes. In contrast, increased TUNEL staining, abnormal nuclear chromatin condensation and kDNA disorganization was observed in venom-treated trypomastigotes, suggesting cell death by an apoptotic mechanism. On the other hand, intracellular amastigotes presented a heterogeneous cell death phenotype profile, where apoptosis-like death seemed to be predominant. Our findings confirm the great potential of *A. mellifera* venom as a source for the development of new drugs for the treatment of neglected diseases such as Chagas disease.

Key words: *Apis mellifera*, *Trypanosoma cruzi*, Chagas disease chemotherapy, programmed cell death, autophagy, apoptosis.

INTRODUCTION

Recognized by the World Health Organization as one of the 13 most neglected tropical diseases in the world, Chagas disease has been a scourge to humanity since antiquity and continues to be a relevant social and economic problem in many Latin American countries (Rassi *et al*. 2009). This life-long infection, also known as American trypanosomiasis, is caused by the protozoan parasite *Trypanosoma cruzi* (Kinetoplastida: Trypanosomatidae) and was discovered in 1909 by the Brazilian physician Carlos Chagas (1879–1934) (Rassi *et al*. 2009). Chagas disease can be transmitted to man by the bite of the insect vector (Hemiptera: Reduviidae) and by non-vectorial mechanisms, such as blood transfusion, vertically from mother to infant, ingestion of food or liquid contaminated with *T. cruzi*, and from accidents in laboratories that deal with live parasites (Moncayo and Silveira, 2009).

Treatment of chagasic patients relies on 2 drugs, Benznidazole and Nifurtimox. These two nitroheterocycles have several limitations, as they are highly toxic and rarely beneficial in the chronic phase of the disease (Urbina and Docampo, 2003). These restrictions encourage the search for alternative synthetic or natural compounds effective for both the clinical treatment of Chagas disease and for chemoprophylaxis on donated blood.

Poisons and toxins found in venomous and poisonous organisms have been the focus of much research over the past 70 years, and much knowledge has been gained in terms of how venoms and their composite toxins give rise to the syndromes associated with envenoming and poisoning (Fox and Serrano, 2007).This has resulted in the development of toxin-based drugs that have already received US Food and Drug Administration approval for use in the United States and in other countries around the world (Fox and Serrano, 2007). Captopril® is an example of a successful venom-based drug for the treatment of hypertension, which inhibits angiotensin-converting enzyme (ACE), and was developed from studies of *Bothrops jararaca* snake venom and its bradykinin-potentiating peptides (BPPs) (Lewis and Garcia, 2003).

Honeybee (*Apis mellifera*) venom contains at least 18 active components with a wide variety of pharmaceutical properties, including enzymes (e.g., phospholipase A_2, hyaluronidase), peptides (e.g., melittin, apamin, MCD peptide), biogenic amines (e.g., histamine, epinephrine) and non-peptide

* Corresponding author: Tel: +55 (21) 2562 6738. Fax: +55 (21) 2560 8344. E-mail: souto.padron@micro.ufrj.br

doi:10.1017/S0031182012000790

components (e.g., free amino acids, lipids and carbohydrates) (Son *et al*. 2007). However, the 2 major bioactive components are melittin, comprising 40–50% of the dry weight of the venom, and PLA_2, comprising 10–12% of the dry weight (Raghuraman and Chattopadhyay, 2007).

Bee venom PLA_2 ($bvPLA_2$) hydrolyses the 2-acyl bonds of phosphatidylcholines, phosphatidylethanolamines, phosphatidylinositols and phosphatidylserines, disrupting membrane integrity and releasing lysophospholipids and fatty acids, which themselves may further damage the membrane (Habermann, 1972). Secretory $bvPLA_2$ may act synergistically with phosphatidylinositol-(3,4)-bisphosphate in affecting membrane integrity and subsequently causing renal carcinoma cell death (Putz *et al*. 2006, 2007). This enzyme also displays bactericidal (i.e., Gram-negative enterobacteria) and trypanocidal (i.e., *Trypanosoma brucei brucei*) activities *in vitro* (Boutrin *et al*. 2008), along with anti-*Plasmodium* toxicity (Moreira *et al*. 2002; Guillaume *et al*. 2004).

Melittin is a highly basic 26-residue peptide that is almost entirely hydrophobic but with a hydrophilic sequence (Lys-Arg-Lys-Arg) near the C-terminus; it is known to damage cell membrane enzyme systems (Habermann, 1972). It induces membrane permeabilization and lyses prokaryotic and eukaryotic cells in a non-selective manner (Papo and Shai, 2003). This mechanism of action is responsible for the haemolytic, anti-microbial (Blondelle and Houghten, 1991; Bechinger, 1997; Diaz-Achirica *et al*. 1998; Chicharro *et al*. 2001; Luque-Ortega *et al*. 2003; Pérez-Cordero, 2011) and anti-tumour (Li *et al*. 2006; Holle *et al*. 2009) activities of melittin.

Several studies have shown the promising effects of crude venom extracts and their isolated components against protozoan parasites, including *Plasmodium falciparum* (Zieler *et al*. 2001), *Leishmania* spp. (Fernandez-Gomez *et al*. 1994; Brand *et al*. 2006; Toyama *et al*. 2006; Passero *et al*. 2007; Tempone *et al*. 2001) and *T. cruzi* (Tempone *et al*. 2007; Gonçalves *et al*. 2002; Ciscotto *et al*. 2009). More recently, our group presented *Crotalus viridis viridis* snake venom as a source for drug development for Chagas disease therapy, as this venom exhibited great efficacy against the intracellular form of the parasite (Adade *et al*. 2011). Following this line of research, in the present study, we have analysed the effect of *A. mellifera* crude venom over the entire *T. cruzi* cycle, investigating the possible venom targets, the effects on the parasite ultrastructure and the parasite death phenotype.

MATERIALS AND METHODS

Parasites

Y strain and CL Brener clone *T. cruzi* epimastigotes were maintained axenically at 28 °C in LIT medium supplemented with 10% fetal calf serum (FCS), with weekly transfers. Four-day-old culture forms, at the mid-log phase of growth, were used in all experiments. Tissue-culture trypomastigotes were obtained from the supernatant of 5- to 6-day-old infected $LLC\text{-}MK_2$ cells maintained in RPMI-1640 medium supplemented with 2% FCS for 5–6 days at 37 °C in a 5% humidified CO_2 atmosphere, as previously described (Adade *et al*. 2011). Intracellular amastigotes were obtained and cultured as described below.

Free parasite treatment

Apis mellifera crude venom was purchased from Sigma Chemical Co. (St Louis, MO, USA). A stock solution (12·5 mg/ml) was prepared in phosphate-buffered saline (PBS, pH 7·2) and stored at −20 °C until use.

Epimastigotes were re-suspended in LIT medium at 2×10^6cells/ml, and an aliquot of 1 ml of the suspension was added to the same volume of *A. mellifera* venom, which had been previously diluted in LIT medium to twice the desired final concentration (0·1 to 200 μg/ml) in 24-well plates (Nunc Inc., Naperville, IL, USA), followed by incubation for 96 h at 28 °C. The number of parasites was determined daily by counting formalin-fixed parasites in a haemocytometer chamber. The parameter used to estimate inhibition of proliferation was the IC_{50}, which corresponds to the drug concentration that inhibited 50% of cell growth. Parasites grown in drug-free LIT medium were used as a control. The growth experiments were carried out in triplicate, and the standard deviation of the cell densities at each time-point are given by error bars. Cell viability was verified by the detection of propidium iodide staining by flow cytometry (described below).

Tissue-culture trypomastigotes were re-suspended to a concentration of 10×10^6cells/ml in RPMI medium (Sigma) containing 10% FCS. This suspension (100 μl) was added to the same volume of the venom that had previously been diluted in RPMI medium to twice the desired final concentration (0·05–200 μg/ml) in 96-well plates (Nunc Inc.), followed by incubation at 37 °C. The parameter LD_{50} (50% trypomastigote lysis) was evaluated by cell counting of formalin-fixed parasites in a haemocytometer chamber after 24 h. The experiments were performed in triplicate.

Cytotoxicity to mammalian cells

Uninfected $LLC\text{-}MK_2$ cells were seeded in 24-well plates (Nunc Inc.) containing glass cover-slips and were maintained with RPMI medium supplemented with 10% FCS and treated or not with 0·1, 0·5, 1, 5

https://doi.org/10.1017/S0031182012000790 Published online by Cambridge University Press

and 10 μg/ ml of the crude venom at 37 °C for 72 h. Each day, the cytotoxic effects were examined using a Trypan blue exclusion test. Briefly, at the end of the incubation period, the glass coverslips were washed with sterile PBS (pH 7·2) and stained with a 1:1 volume dilution of trypan blue solution: RPMI for 5 min. After this period, the cells were gently washed with PBS and observed using a Zeiss Axiovert light microscope (Oberkochen, Germany). At least 500 cells per well were examined, enabling the determination of the LC_{50} value (i.e., the venom concentration that caused a 50% reduction in cellular viability). In addition, uninfected mouse peritoneal macrophages were seeded in 96-well plates (Nunc Inc.), maintained in RPMI medium and treated or not with 1 and 5 μg/ ml of the crude venom at 37 °C for 48 h. After this period, the cytotoxic effects were examined using a MTS (3-(4,5-dimethylthiazol-2-yl)-5-(3-carboxymethoxyphenyl)-2-(4-sulfophenyl)-2H-tetrazolium, inner salt) assay, in which the reduction of MTS in soluble formazan by mitochondrial dehydrogenase enzymes occurs only in healthy and metabolically active cells (Berridge *et al*. 2005). Briefly, at the end of the incubation period, the cells were washed with sterile PBS (pH 7·2), the wells filled with RPMI medium (without a pH indicator colour), 10 mM glucose and 20 μl of MTS/ PMS reagent (20:1), for which the stock solution was 2 mg/ ml MTS and 0·92 mg/ml PMS prepared in DPBS (Promega, Madison, WI, USA). The absorbance was evaluated in a microplate reader spectrophotometer at 490 nm, after a 3-h incubation, during which the toxicity was measured. All the animal experimentation protocols were submitted to and approved by the Commission of Evaluation of the Use of Research Animals (Comissão de Avaliação do Uso de Animais em Pesquisa (CAUAP) of the Biophysics Institute Carlos Chagas Filho. Both experiments were carried out in triplicate.

Treatment over the T. cruzi *intracellular cycle*

To investigate the effect of *A. mellifera* venom on the intracellular cycle of the parasite, LLC-MK_2 cells were seeded in 24-well plates containing glass coverslips, cultivated in RPMI supplemented with 10% FCS, and maintained at 37 °C in a 5% CO_2 humidified atmosphere for 1 day as previously described (Adade *et al*. 2011). Thereafter, the cultures were washed and infected with tissue-culture trypomastigotes (parasite:host cell ratio 10:1). After 24 h of interaction, non-internalized parasites were removed by repeated washes with PBS, and the cells were cultivated in fresh RPMI medium containing 2% FCS with (0·025–0·4 μg/ml) or without bee venom. Media were changed every 2 days. Coverslips were collected daily up to 96 h, rinsed in PBS, fixed in Bouin's solution, stained with Giemsa and mounted on glass slides with Permount (Fisher Scientific, New Jersey, USA). Parasite infection was quantified using a Zeiss Axioplan 2 light microscope (Oberkochen, Germany) equipped with a Color View XS digital video camera. The number of intracellular amastigotes per infected cell and per 100 cells was evaluated by counting a total of 500 cells in 3 different experiments. The IC_{50} was estimated as the dose that reduced the number of amastigotes per infected cell by 50%.

Scanning electron microscopy

Epimastigotes treated with 0·67 μg/ml and tissue-culture trypomastigotes treated with 0·1 μg/ml of the crude bee venom for 1–24 h were washed twice with PBS and fixed for 1 h with 2·5% glutaraldehyde (GA) in 0·1 M cacodylate buffer (pH 7·2), 5 mM calcium chloride and 2% sucrose. The parasites were then washed with the same buffer and adhered to glass coverslips coated with 0·1% poly-*L*-lysine (M.W. 70 000, Sigma). After post-fixation for 15 min with 1% osmium tetroxide (OsO_4) containing 0·8% potassium ferrocyanide and 5 mM calcium chloride in cacodylate buffer 0·1 M (pH 7·2), cells were washed, dehydrated in graded ethanol and then critical-point dried with CO_2. Samples were adhered to scanning electron microscopy stubs, coated with a 20 nm-thick gold layer in a sputtering device and then observed in a JEOL JSM 5310 scanning electron microscope (Tokyo, Japan) operating at 25 kV. Digital images were acquired and stored in a computer.

Transmission electron microscopy

Epimastigotes and trypomastigotes treated with their respective IC_{50} and LD_{50} of *A. mellifera* venom for 24 h, and the infected LLC-MK_2 cells treated with 0·125 μg/ml venom for 72 h were fixed as described above. After fixation, LLC-MK_2 cells were gently scraped off with a rubber policeman and harvested by centrifugation. All samples were post-fixed in 1% osmium tetroxide (OsO_4) containing 0·8% potassium ferrocyanide and 5 mM calcium chloride in 0·1 M cacodylate buffer (pH 7·2) for 1 h at room temperature, dehydrated in graded acetone, embedded in PolyBed812 (Polysciences Inc., Warrington, PA, USA), and then polymerized for 3 days at 60 °C. Ultra-thin sections obtained with a Leica (Nussloch, Germany) ultramicrotome were stained with uranyl acetate and lead citrate and observed in a FEI Morgagni F 268 (Eindhoven, The Netherlands) transmission electron microscope operating at 80 kV.

Flow cytometry analysis

Epimastigotes (maintained in LIT medium at 28 °C) and tissue-culture trypomastigotes (maintained in RPMI medium at 37 °C) were treated (at 1×10^6

https://doi.org/10.1017/S0031182012000790 Published online by Cambridge University Press

cells/ml) with 0·335–1·34 or 0·05–0·2 μg/ml *A. mellifera* venom, respectively, for 1 day. The parasites were then incubated with 15 μg/ml propidium iodide (PI) plus 10 μg/ml rhodamine 123 (Rh123) for 15 min. Changes in the Rh123 fluorescence level between treated and untreated parasites were quantified using an arbitrary index of variation (IV) obtained by the equation (MT − MC)/MC, where MT is the median of fluorescence for treated parasites and MC that of untreated parasites. Negative IV values corresponded to depolarization of the mitochondrial membrane.

Both parasite morphological forms (1×10^6/ml), treated for 24 h or not, were evaluated for DNA fragmentation by the terminal deoxynucleotidyl-transferase-mediate fluorescein dUTP nick end labelling technique (TUNEL) using the APO-BrdU™ TUNEL Assay Kit (Molecular Probes Inc.) to detect apoptotic cells, according to the manufacturer's specifications. Treated parasites were analysed immediately. The positive control was a fixed human lymphoma cell line that was included in the TUNEL Assay kit.

In all the performed assays, the cells were kept on ice until data acquisition and analysis with a FACSCalibur flow cytometer (Becton-Dickinson, Franklin Lakes, NJ, USA) equipped with CellQuest software (Joseph Trotter, Scripps Research Institute, San Diego, CA, USA). A total of 10 000 events were acquired in the region previously established as the region that corresponded to the parasites. All flow cytometry analyses were done in at least 3 independent experiments.

Fluorimetry

T. cruzi epimastigotes and trypomastigotes were treated with bee venom (0·335–0·67 and 0·05–1 μg/ml, respectively) or not (control cells) for 24 h, washed with PBS (pH 7·2) and incubated with 100 μM of monodansyl cadaverine (MDC) (Sigma-Aldrich) for 1 h at 28 °C (epimastigotes) or 37 °C (trypomastigotes), avoiding light incidence. After this period, the parasites were washed twice in PBS and fixed with 2% formaldehyde (FA) freshly prepared from paraformaldehyde for 20 min at room temperature. Each condition was performed in triplicate and added to different wells (100 μl final volume) of a black 96-well plate and analysed in a Molecular Devices Microplate Reader (a SpectraMax M2/M2^e spectrofluorometer) using 355 and 460 nm wavelengths for excitation and emission, respectively. Suspensions of 2% FA and 2% FA plus 100 μM MDC were also made as reaction controls and were simultaneously read in the plate.

Fluorescence microscopy

The cell death analysis in intracellular amastigotes was carried out using TUNEL technique and MDC staining. For both analyses, LLC-MK$_2$ cells were seeded in 24-well plates containing glass coverslips, cultivated and infected as cited above. The cells were cultivated for 3 days in fresh RPMI medium containing 2% FCS with 0·125 μg/ ml or without *A. mellifera* venom. Media were changed daily. TUNEL was performed using the same kit used for flow cytometry analysis, and a positive control was established by infected cells treated for 45 min at room temperature, with 2·5 μg/ ml DNAse I (Sigma) prior to the procedure. After this period, all the samples were washed twice with PBS, fixed for 20 min at 4 °C with 4% FA and processed according to the manufacturer's specifications. After staining, cells were further incubated with 10 μg/ ml 4,6-diamidino-2-phenylindole (DAPI), for nuclei and kinetoplast visualization. For MDC staining, all samples were washed twice with PBS, incubated for 1 h with 100 μM MDC at 37 °C and fixed for 20 min at 4 °C with 4% FA. At the end of this period, the cells were further incubated with a PI solution (10 μg/ ml) for 15 min to facilitate the nuclei and kinetoplast detection. All the samples were washed twice with PBS, mounted on glass slides with 0·2 M N-propyl gallate to reduce fading and analysed by Zeiss Axioplan 2 microscope equipped with epifluorescence. The number of parasites per infected cell, and the percentage of TUNEL- and MDC- positive parasites were scored in 300 host cells per slide.

Evaluation of intracellular amastigotes autophagy

LLC-MK$_2$ cells were seeded in 24-well plates containing glass coverslips, cultivated and infected as cited above. Prior to the *A. mellifera* treatment with 0·125 μg/ ml, cell cultures were incubated or not with 10 mM 3-methyladenine (3-MA, Sigma-Aldrich). After 3 days, the coverslips were collected, rinsed in PBS, fixed in Bouin's solution, stained with Giemsa and mounted on glass slides with Permount (Fisher Scientific). The number of intracellular amastigotes per infected cell was evaluated by counting a total of 500 cells in 2 different experiments.

Statistical analysis

Mean value comparisons between the control and treated groups were performed using the Kruskal-Wallis test in the BioEstat 2.0 program for Windows. Differences with $P \leqslant 0{\cdot}05$ were considered statistically significant.

RESULTS

Treatment of epimastigotes with *A. mellifera* venom resulted in dose-dependent growth inhibition (Table 1), with an IC$_{50}$/ 1 day treatment of

https://doi.org/10.1017/S0031182012000790 Published online by Cambridge University Press

Table 1. Effect of *Apis mellifera* venom on the three evolutive forms of *Trypanosoma cruzi* (CL Brener clone)

(IC_{50} and LD_{50} values are expressed in μg/ml. Selectivity index (SI)[e] was determined by the ratio between LC^{f}_{50}/IC_{50} or LD_{50} values. Data are expressed as means ± standard deviation of 3 independent experiments.)

[a]	Epimastigotes [b]*	Trypomastigotes[c]	Intracellular amastigotes[d]
1	0·67 ± 0·25 (15)[e]	0·10 ± 0·03 (100)	0·158 ± 0·03 (63·3)
2	0·38 ± 0·00 (26·3)	nd	0·197 ± 0·11 (50·8)
3	0·33 ± 0·07 (30·3)	nd	0·125 ± 0·09 (80)
4	0·29 ± 0·11 (34·5)	nd	0·117 ± 0·06 (85·5)

[a] Days of treatment.
[b] IC_{50} venom concentration to inhibit 50% parasite growth each day.
[c] LD_{50} venom concentration that lyses 50% of trypomastigote cultures.
[d] IC_{50} venom concentration to reduce by 50% the number of intracellular amastigotes per infected cell.
[e] SI values, where $LC_{50} > 10\,\mu$g/ml.
[f] LC_{50} venom concentration that lyses 50% of LLC-MK_2 cells.
nd,Not done.

0·85 ± 0·05 and 0·67 ± 0·25 μg/ ml for the Y strain and CL Brener clone, respectively. Because those results were not statistically different ($P > 0·05$), all other experiments with epimastigote forms were performed with CL Brener parasites and utilizing the 0·67 μg/ ml concentration for a 24-h treatment. Incubation of parasites with 12·6–200 μg/ ml *A. mellifera* venom led to 100% cell death soon after the first 24 h of treatment. Treatment of tissue-culture trypomastigotes also induced lysis of the parasites, with an LD_{50}/ 1 day value of 0·10 ± 0·03 μg/ ml (Table 1).

Parasites treated for 1 day with 0·67μg/ ml (epimastigotes; Fig. 1B–F) and 0·1 μg/ml (trypomastigotes; Fig. 1H, I) presented morphological alterations that were observed by scanning electron microscopy (SEM) (Fig. 1). The parasites presented loss of cell body membrane integrity (Fig. 1B–F; H, I), with the presence of variable size pores (Fig. 1B inset, F, H) and membrane shrinkage (Fig. 1F). Both parasite forms presented variable amounts and abnormal membrane blebbing in the flagellar and cell body membranes (Fig. 1C, H inset), although cell body retraction was also commonly detected in treated trypomastigotes (Fig. 1I). Only those parasites that displayed broken flagella did not present significant alterations in body shape (Fig. 1C, D).

Analysis of venom-treated epimastigotes by transmission electron microscopy (TEM) showed changes in the morphology of the reservosomes, characterized by the swelling of the organelle and the loss of their electron-dense matrix and internal vesicles (Fig. 2B, H). An intense swelling of the mitochondria (Fig. 2C, E), with an altered inner mitochondrial membrane forming concentric membrane structures inside the organelle, was also observed (Fig. 2B,C, E). Despite mitochondrial damage, the kDNA network preserved its typical morphology (Fig. 2C, D). One remarkable feature of epimastigote treatment was the presence of endoplasmic reticulum profiles surrounding different structures, suggesting autophagosome formation (Fig. 2D, G, H). Intense cell shape disorganization with large cell body projections was frequently observed (Fig. 2F).

The most striking morphological effect of *A. mellifera* venom treatment on trypomastigotes was mitochondrial swelling, with disorganization of the internal membranes and a retraction of mitochondrial kDNA filaments (Fig. 3B–E, G, H). Unlike what was observed in treated epimastigotes, trypomastigotes presented a remarkable kDNA network alteration characterized by the fragmentation of DNA filaments (Fig. 3B–E, G). The venom treatment also led to a strong nuclear envelope dilatation (Fig. 3G, H), increased nuclear chromatin condensation (Fig. 3G, H), detachment of the plasma membrane and the presence of blebs budding from the cell body and flagellar membranes (Fig. 3C, D and inset in G), swelling of cytoplasmic vacuoles (Fig. 3B) and altered lysosome-related organelles with loss of their contents through leaking (Fig. 3F).

To investigate *A. mellifera* venom activity against the *T. cruzi* intracellular form, we tested the bee venom cytotoxicity to the host cells, which involved treating LLC-MK_2 cells with 0·1, 0·5, 1, 5 and 10 μg/ ml for 72 h and examining treated cells with a Trypan blue cell viability test (data not shown). The positive (blue) staining indicated non-viable cells. The 0·1–5 μg/ml treatment after 24 h of incubation induced less than a 20% loss of cell viability, whereas nearly 42% of cell viability was lost with the 10 μg/ml treatment. Following treatment, the 5 μg/ml incubation increased cell damage to 32% and 40% after 48 and 72 h, respectively. Incubation in the presence of 10 μg/ ml reduced cellular viability in 61% and 86% of cells after 48 and 72 h, respectively, indicating remarkable cell damage. In parallel, to investigate the cytotoxicity of the venom in primary host cell cultures, we tested the activity of the venom in peritoneal macrophages (data not shown). The cells were treated with 1 and 5 μg/ ml for 48 h and were examined with an MTS assay. The formazan

https://doi.org/10.1017/S0031182012000790 Published online by Cambridge University Press

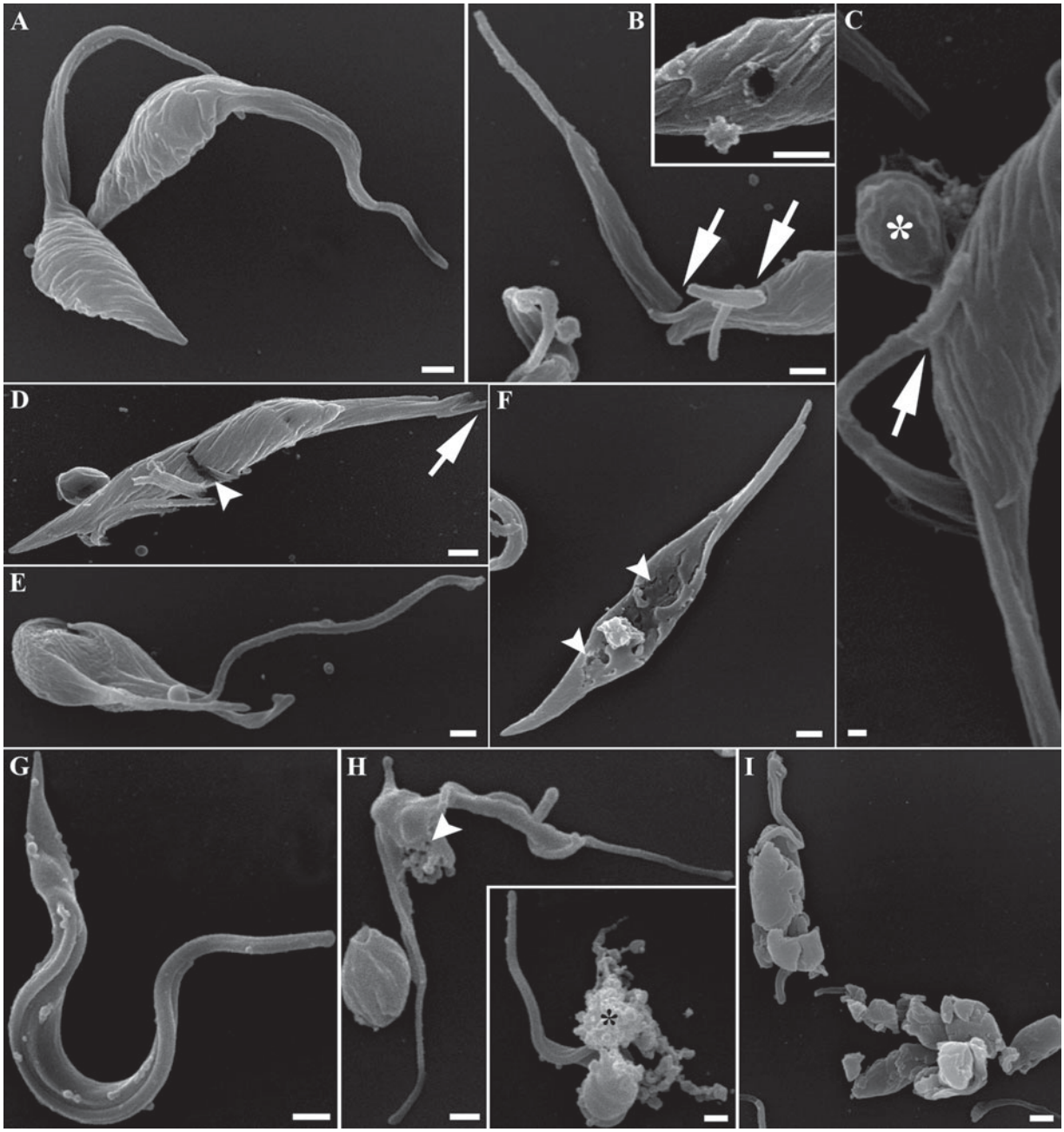

Fig. 1. Scanning electron microscopy of control epimastigotes (A), trypomastigotes (G) and treated epimastigotes (B–F) and trypomastigotes (H,I) displaying remarkable alterations. Loss of cell body membrane integrity with cracks (arrowhead in D), variable sized pores (arrowheads in F, H and inset in B), abnormal conformation of the cell body (asterisk in C and E, H,I), membrane shrinkage (F) and broken flagella (arrows in B–D) were the most common alterations. Abnormal membrane blebbing (asterisks) from the cell body was also detected in both parasite forms (H- inset). Scale bars: 1 μm.

precipitate occurred through the action of mitochondrial dehydrogenase enzymes in most treated cells, with no significant reduction in absorbance ($P \leqslant 0{\cdot}05$) after the 5μg/ ml treatment compared to control cells.

The effect of bee venom on intracellular amastigotes was analysed in infected LLC-MK_2cells. After 24 h of infection, cells were treated with 0·025–0·4 μg/ ml of *A. mellifera* venom for up to 96 h, and the numbers of parasites per infected cell and per 100 cells were quantified daily by light microscopy. Untreated infected cells exhibited a higher infection profile compared to treated cells, with a large number of intracellular amastigote forms present on all analysed days. In contrast, treated infected cells had reduced numbers of both amastigotes per cell and per 100 cells with the different venom concentrations and at the different treatment times. The reduction in the numbers of parasites per infected cell varied from 53% to 73% after 24 or 96 h of treatment, respectively. A greater reduction was observed in the number of parasites per 100 cells, which was approximately 95%

https://doi.org/10.1017/S0031182012000790 Published online by Cambridge University Press

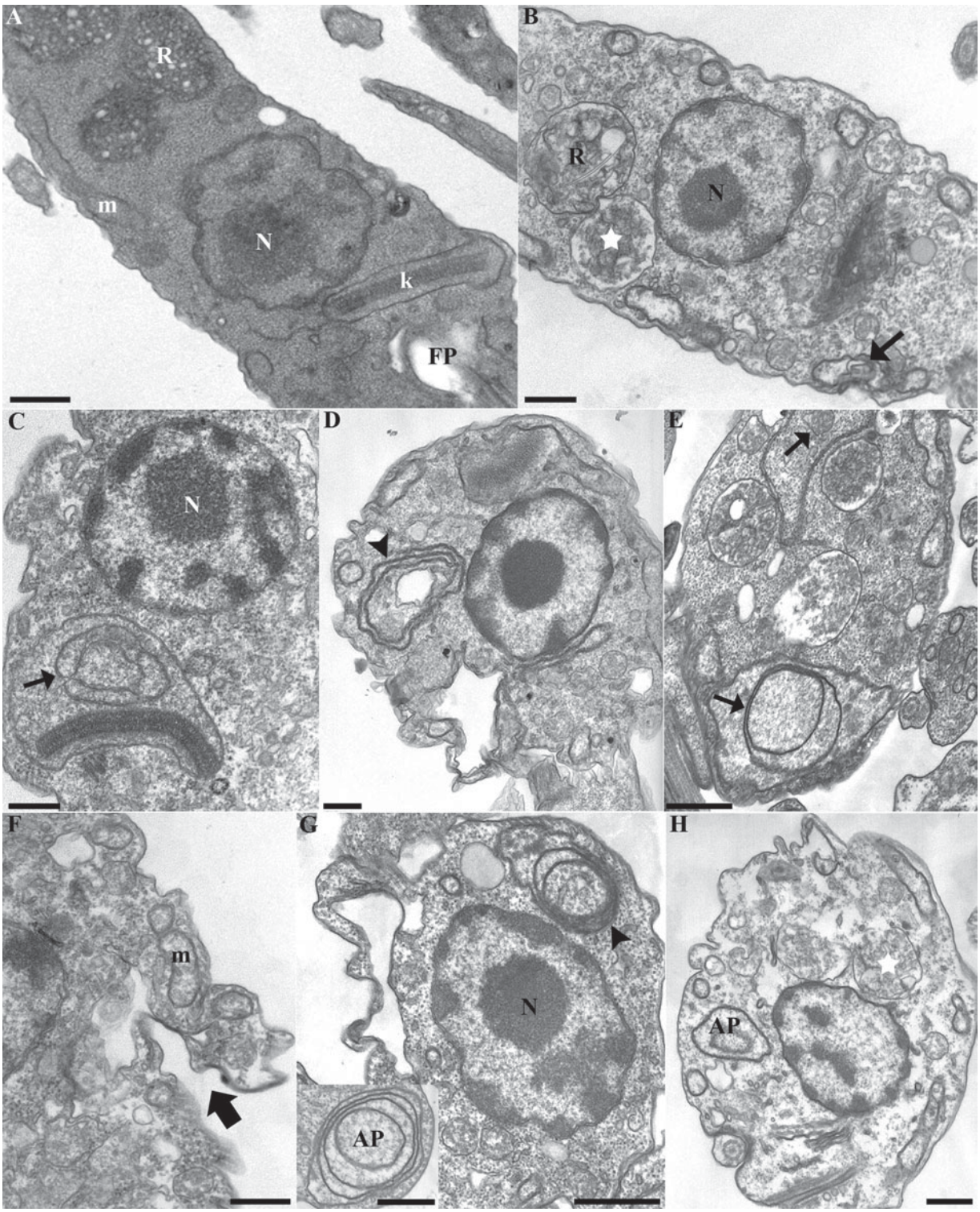

Fig. 2. Transmission electron microscopy (TEM) of untreated epimastigotes (A) and treated parasites exhibiting remarkable alterations (C–H). Control cells (A) displayed typical elongated cell bodies, flagellar pocket (FP), mitochondria (m), kinetoplast (k), reservosomes (R), and nucleus (N). The venom-treated epimastigotes (C–H) presented different alterations on mitochondria, such as swelling (C) and altered inner membranes with concentric figure formations (thin arrows in B,C, E). No altered kinetoplasts were observed (C,D). The highlighted features were the presence of endoplasmic reticulum profiles surrounding different structures (arrowheads in D, G) suggesting autophagosome (AP) formation, a remarkable autophagy-like death indication. Other detected alterations were disorganized reservosomes (white star in B) and plasma membrane projections (thick arrow in F). Scale bars: 0·5 μm.

after 24 or 96 h of treatment. The IC_{50} value to inhibit the proliferation of intracellular amastigotes in the presence of the venom was 0·158 ± 0·03 μg/ ml when analyed after 24 h and reached 0·117 ± 0·06 μg/ ml on the last day of treatment (Table 1). The IC_{50} and LD_{50} values allowed quantification of the

https://doi.org/10.1017/S0031182012000790 Published online by Cambridge University Press

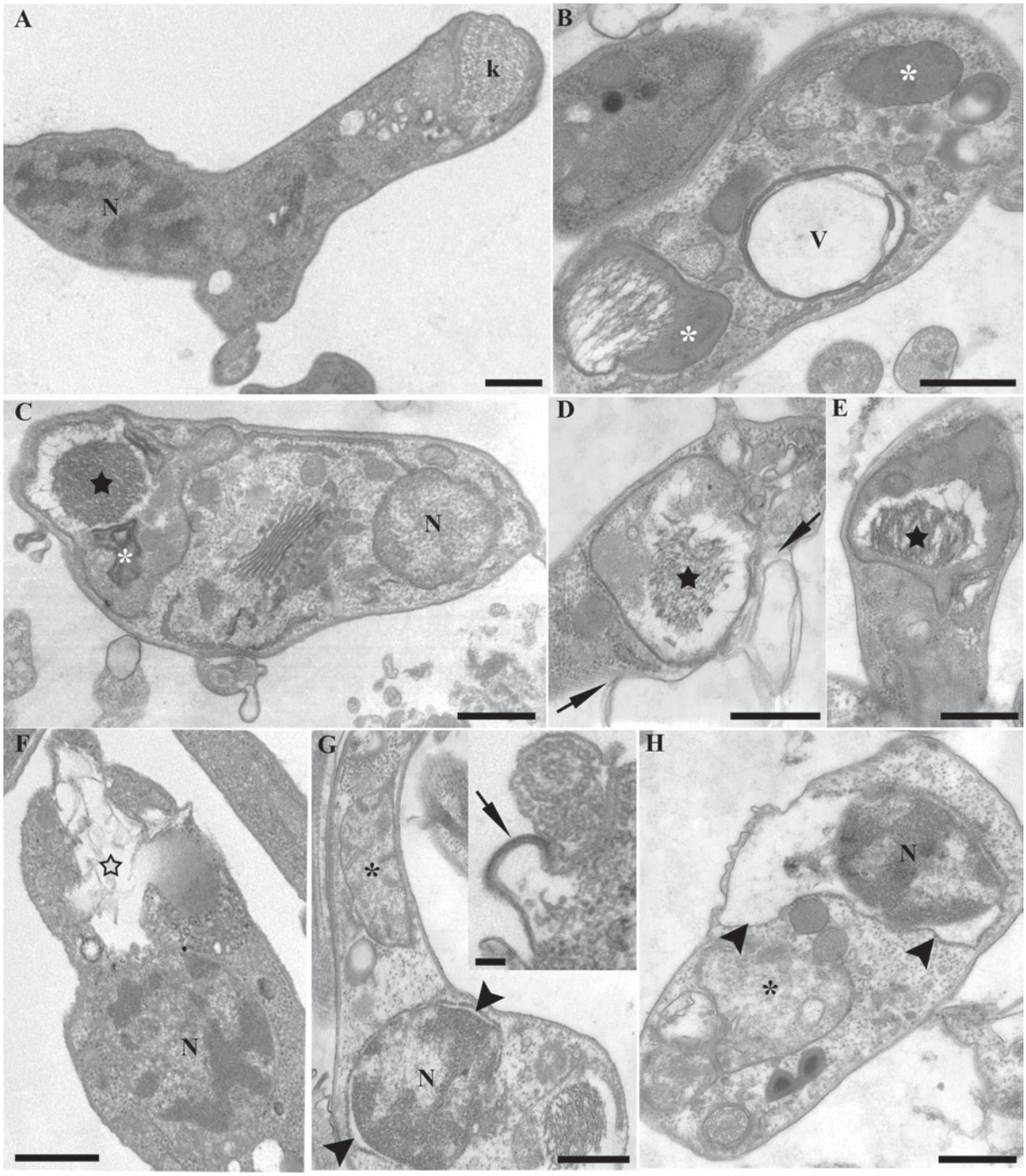

Fig. 3. Transmission electron microscopy (TEM) of untreated (A) and venom-treated trypomastigotes (B–H). Control trypomastigote (A) exhibiting normal organelles, such as full plasma membrane, nucleus (N) and kinetoplast (k). Treated trypomastigotes (B–H) exhibited membrane extensions in the cell body (arrows in D, G inset), swollen vacuoles (V) and mitochondria with strong condensation of the internal membrane (asterisk in B), concentric figures (asterisk in C) and increased swelling (asterisk in H). Additionally, the treated trypomastigotes presented a strongly altered kDNA network with an apparent retraction from the mitochondria content (black stars in C–E). They presented apoptosis-like features, such as strong nuclear envelope dilatation (arrowheads in G,H) with increased nuclear chromatin condensation (G,H) and absence of endoplasmic reticulum profiles or autophagosomes. Some treated parasites exhibited lysosome-related organelles (empty stars in F) that lost their contents due to leaking. Scale bars: 0·5 μm.

selectivity index (SI) when related to the LC_{50}. The most active treatment was against trypomastigotes, which also displayed the highest SI value (100-fold), followed by the intracellular amastigote treatment, which rose 80-fold after 72 h of incubation (Table 1).

To analyse the effect of the venom on the morphology of intracellular amastigotes, LLC-MK_2cells were infected, treated for 72 h with 0·125μg/ ml and processed for light and transmission electron microscopy. In non-treated cells, the

https://doi.org/10.1017/S0031182012000790 Published online by Cambridge University Press

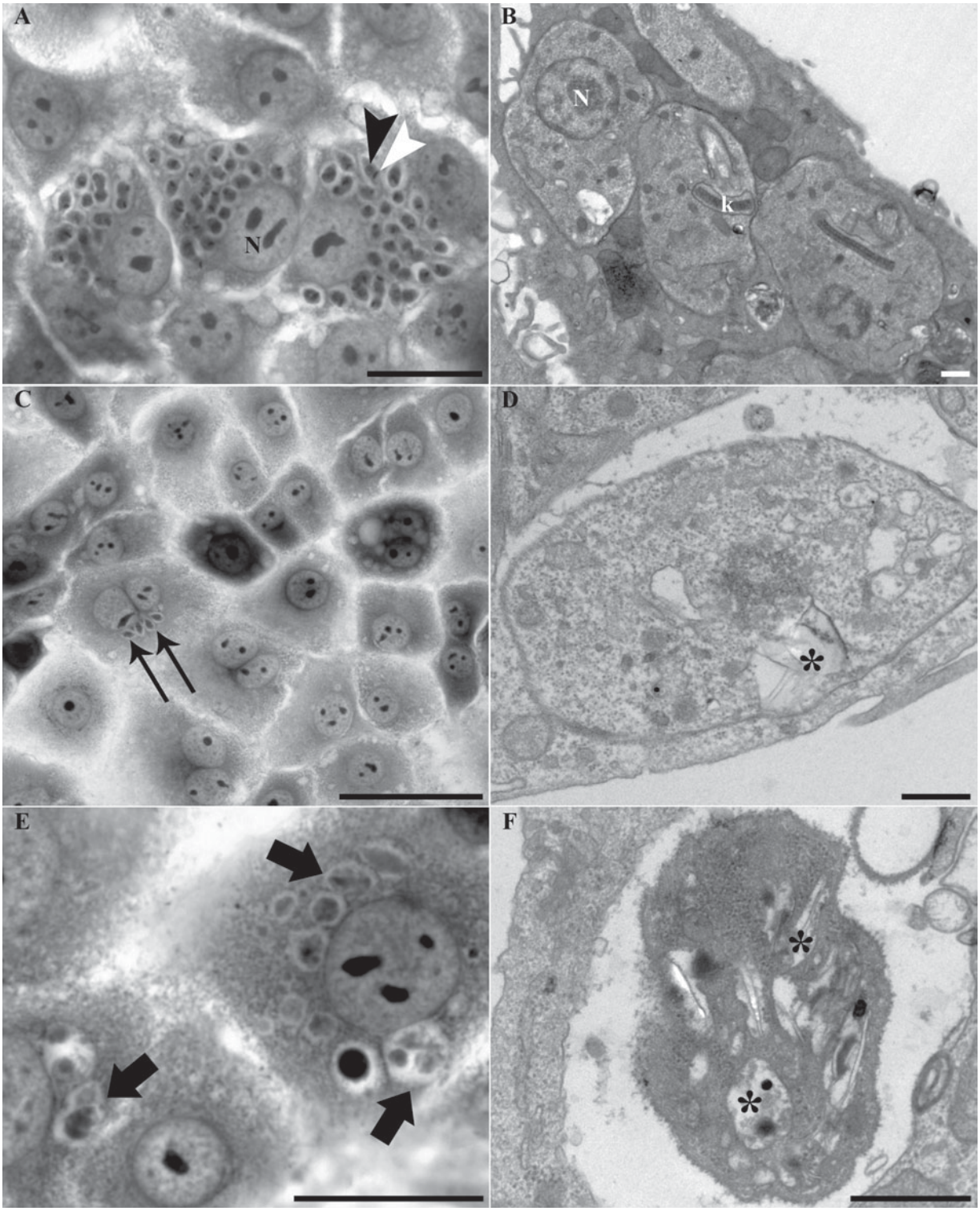

Fig. 4. Light (A, C, E) and transmission electron microscopy (B, D, F) of *Trypanosoma cruzi*-infected and treated LLC-MK_2 cells. (A–B) Untreated cells exhibited a high number of intracellular amastigotes presenting round body shape with typical nucleus (black arrowhead) and bar-shaped kinetoplast (white arrowhead). This normal morphology was confirmed by TEM, by which intracellular parasites presented with typical nucleus (N) and kinetoplast (k). The treatment resulted in a low infection index, confirmed by the low number of normal amastigotes (C, thin arrows) detected inside treated host cells. Occasionally, detection of altered intracellular amastigotes by light (E) and electron microscopy was possible (D–F). Ultrastructural analysis revealed amastigotes exhibiting disorganized internal structures in their cell bodies (asterisks). Scale bars: A, C, E: 20 μm; B, D, F: 0·5 μm.

parasites that existed inside the host cell cytoplasm exhibited typical morphologies (Fig. 4A, B), such as rounded body shapes and bar-shaped kinetoplasts. Through ultrastructural analysis, it was possible to verify the aspects of other organelles, such as the nucleus, the mitochondria, and the short flagellum

https://doi.org/10.1017/S0031182012000790 Published online by Cambridge University Press

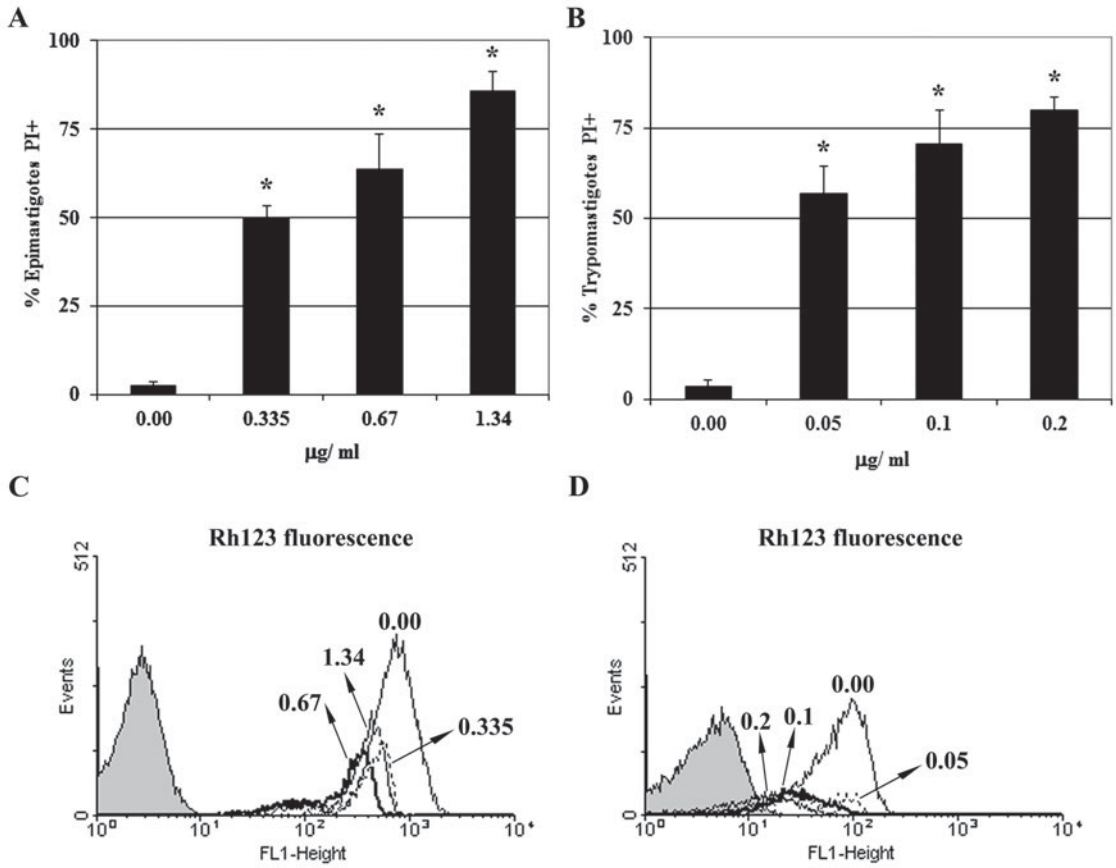

Fig. 5. Flow cytometry analysis of treated epimastigotes (A, C) and trypomastigotes (B, D) stained with propidium iodide (PI) (A, B) and rhodamine 123 (Rh 123) (C, D). The rising percentage of PI labelling indicates loss of parasite viability at different concentrations. Data are expressed as means ± standard deviation of 3 different experiments, and asterisks indicate significant differences compared to untreated parasites. The decrease in Rh 123 fluorescence emission indicates altered mitochondrial membrane potential, where histograms (thick black lines) display parasites treated with their respective IC_{50} (A) and LD_{50} (B) values ($P \leqslant 0{\cdot}05$).

(Fig. 4B). The low infection index of infected and treated LLC-MK_2 cells was confirmed. Some intracellular parasites with abnormal morphologies (Fig. 4E) resulted from the venom treatment. TEM confirmed that intracellular amastigotes presented with morphological alterations, such as swelling of their cell bodies and changes in lysosome-related organelles (LRO), which was characterized by swelling and by the presence of an increased number of electron-dense rod-shaped bodies (Fig. 4D, F).

Because ultrastructural changes observed in all developmental forms after *A. mellifera* treatment were suggestive of membrane damage and loss of cell viability with distinct cell death phenotypes, we proceeded with flow cytometry analysis utilizing propidium iodide (PI) and rhodamine 123 (Rh 123) staining (Fig. 5A, B; Table 2). Parasites exhibited a high percentage of PI-labelled cells, which reached 67·2% (epimastigotes) and 79·7% (trypomastigotes) when treated with IC_{50} and LD_{50} concentrations, respectively, of bee venom. The flow cytometry data also confirmed the strong mitochondrial alterations detected by TEM, suggesting interference in the proton electrochemical potential gradient membrane in venom-treated and Rh 123-stained parasites. Treated epimastigotes and trypomastigotes exhibited gradual decreases in Rh 123 median fluorescence emission, with IV reaching −0·46 and −0·32 at IC_{50} and LD_{50} doses, respectively (Fig. 5C, D; Table 2).

As previously mentioned, after venom treatment, epimastigotes frequently presented concentric endoplasmic reticulum profiles, sometimes surrounding different structures resembling autophagosomes, which are a remarkable feature of the autophagic death phenotype. However, such structures were virtually absent in treated trypomastigotes. To confirm our suspicions, both treated *T. cruzi* developmental forms were incubated with MDC, a fluorescent autophagy marker, and analysed by fluorimetry (Fig. 6A, C). The MDC emission fluorescence by treated epimastigotes (0·67 µg/ ml) was significantly greater ($P \leqslant 0{\cdot}05$) than those observed in untreated parasites, even when a lower venom concentration (0·335 µg/ ml) was used (Fig. 6A). However, trypomastigotes treated with 0·05 and 0·1 µg/ ml displayed low and no significant ($P > 0{\cdot}05$) MDC fluorescence emission in relation to the untreated parasites (Fig. 6C). The fluorescence

https://doi.org/10.1017/S0031182012000790 Published online by Cambridge University Press

Table 2. Flow cytometry analysis of *Trypanosoma cruzi* treated with *Apis mellifera* venom labelled with PI and Rh123

(*A. mellifera* venom treatment was for 1 day in LIT at 28 °C for epimastigotes and in RPMI at 37 °C for trypomastigotes.)

	μg/ml	PI[b] (%)	Median Rh123	IV[a]
Epimastigotes	0	2·56	693·6	0·00
	0·335	48·6	438·8	−0·37
	0·67	67·2	370·5	−0·46
	1·34	89·5	344·9	−0·50
Trypomastigotes	0	0·85	165·5	0·00
	0·05	75·5	119·7	−0·27
	0·1	79·7	111·4	−0·32
	0·2	83·0	105·0	−0·36

[a]Arbitrary Index of Variation – IV = (MT-MC)/MC, where MT corresponds to the median of the fluorescence for treated parasites and MC to that of control parasites.
[b]Percentage of PI-positive cells.
[c]Data represent the means ± standard deviation of at least 3 independent experiments.

intensity observed in the venom-treated trypomastigotes at the LD_{50} was approximately 10 times lower than that observed in the epimastigotes at their IC_{50}.

The remarkable ultrastructural changes of trypomastigotes after incubation with *A. mellifera* venom (Fig. 3B–E) included not only nuclear DNA fragmentation but also an effect on the kDNA filaments, neither of which were observed in epimastigotes. These data were confirmed by *in situ* labelling of DNA fragments (TUNEL assay), where it was much more evident in treated trypomastigotes (Fig. 6D) than in epimastigotes (Fig. 6B). Only 17·9% of epimastigotes treated with 0·67 μg/ ml *A. mellifera* venom were TUNEL-positive, compared to 70·7% of trypomastigotes treated with 0·1 μg/ml venom. Further, only 3·7% of epimastigotes treated with 0·335 μg/ml venom (half IC_{50}) were TUNEL-positive, compared to 18% of trypomastigotes treated with 0·05 μg/ml venom (half LD_{50}).

Since ultrastructural analysis of amastigotes did not indicate a preferential cell death pathway, we then performed analysis of venom-treated parasites using TUNEL assay (Fig. 7) and MDC staining (Fig. 8). In parallel, we decided also to perform the treatment of infected LLC-MK_2 in the presence of 3-MA, a well-known autophagy-like cell death inhibitor by suppressing autophagosomes formation (Levine and Yuan, 2005), and quantify the number of intracellular parasites per infected cell (Fig. 8D).

The TUNEL assay revealed a great number of positive parasites after *A. mellifera* treatment. The positive fluorescence staining exhibited by venom-treated amastigotes (Fig. 7 D–F) was very similar to that observed with DNAse-treated parasites (Fig. 7 A–C). The *in situ* labelling of DNA fragments was detected both at the kinetoplast and nucleus (Fig. 7F; coloured green) and the percentage of venom-treated parasites stained by TUNEL was 45·4 ± 2·1 (Fig. 7H), whereas 56·6 ± 8·1% was observed with DAPI stain after DNAse treatment. There was no statistical difference between these two samples ($P > 0·05$). However, some intracellular amastigotes were not stained by TUNEL reaction, even within the same host cell. Thus, we investigated the autophagy-like cell death occurrence in those intracellular parasites (Fig. 8). Venom-treated intracellular amastigotes exhibited 28·3 ± 7·8% MDC-positive staining (Fig. 8 C, E), whereas untreated parasites exhibited 7·8 ± 2·4% MDC-positive staining (Fig. 8 E). This difference was statistically significant ($P \leqslant 0·05$). Death by autophagy was also evaluated by assessing the intracellular growth of parasites (Fig. 8D). In venom-treated LLC-MK_2 cells, we observed a 52% reduction in the number of intracellular parasites. When cells were incubated in the presence of *A. mellifera* venom plus the inhibitor 3-MA, the reduction growth was of 34%, showing that 3-MA reverses the cell death at least partially (Fig. 8D). These data are statistically different ($P \leqslant 0·05$) confirming the autophagy-like cell death phenomenon.

The data set obtained with the use of ultrastructural techniques and fluorescent markers strongly suggests that the mechanisms of cell death triggered by the venom of *A. mellifera* in all developmental *T. cruzi* forms are mostly autophagy and apoptosis, respectively.

DISCUSSION

Natural products (such as animal venom) and their derivatives represent more than 30% of pharmaceuticals currently on the market (Kirkpatrick, 2002) and are the major sources of innovative therapeutic agents for diseases caused by bacteria, parasites and fungi (Altmann, 2001). Following this approach, animal venom (mostly from snakes) has been screened as potentially useful for the treatment of neglected diseases caused by parasites, including Chagas disease (Ciscotto *et al*. 2009; Gonçalves *et al*. 2002; Tempone *et al*. 2001; Adade *et al*. 2011) and Leishmaniasis (Fernandez-Gomez *et al*. 1994; Brand *et al*. 2006; Toyama *et al*. 2006; Passero *et al*. 2007; Tempone *et al*. 2007).

The therapeutic application of honeybee venom for the chemotherapy of various diseases is known as bee venom therapy (Son *et al*. 2007) and has mainly been used to treat arthritis (Park *et al*. 2004), rheumatism (Kwon *et al*. 2002), back pain (Chen *et al*. 2006) and cancerous tumours (Huh *et al*. 2010; Park *et al*. 2011). However, despite the information available about the pharmaceutical properties of *A. mellifera* venom, no studies had previously been performed to evaluate the effect of crude venom on parasitic protozoa. Only

https://doi.org/10.1017/S0031182012000790 Published online by Cambridge University Press

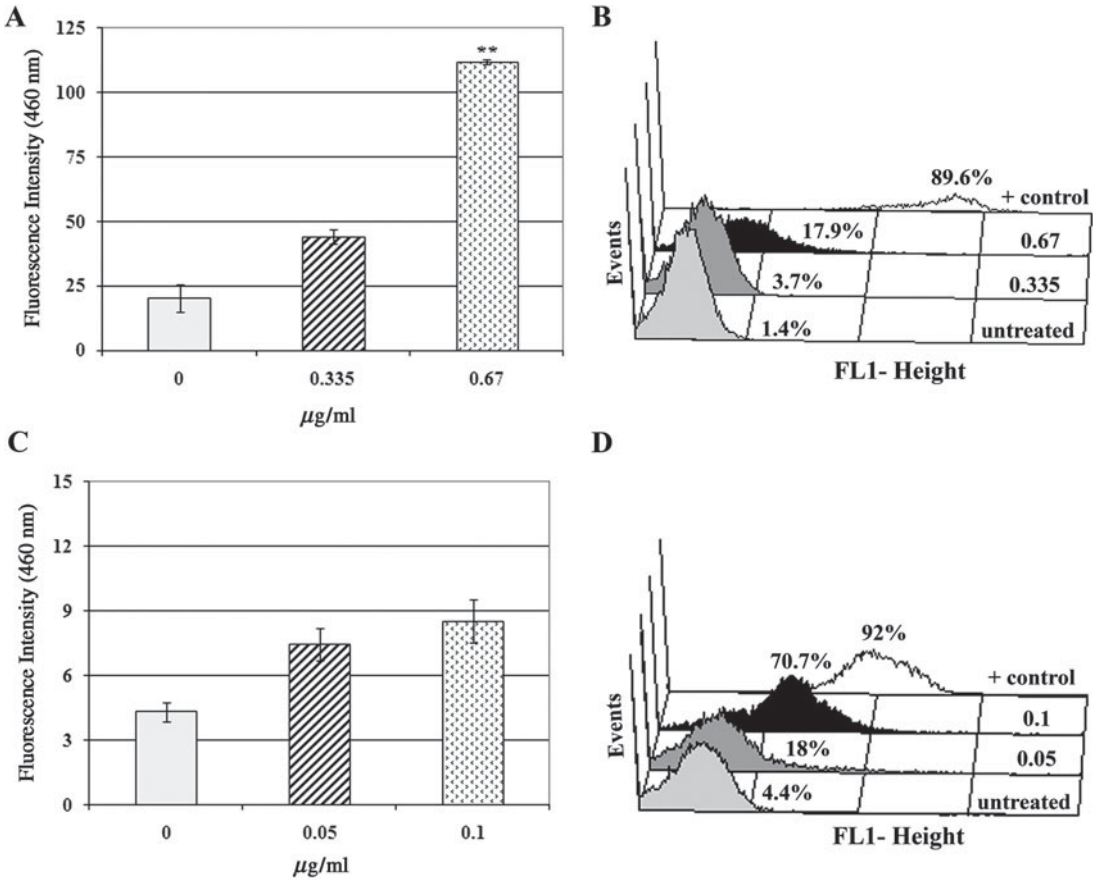

Fig. 6. Fluorimetric analysis of MDC (A, C) and TUNEL (B, D) labelling in treated *Trypanosoma cruzi* epimastigotes (A, B) and trypomastigotes (C, D). The MDC reading was done in a microplate reader using wavelengths at 355 and 460 nm for excitation and emission, respectively. Asterisks indicate significant differences related to untreated parasites ($P \leqslant 0{\cdot}05$). Note that treated epimastigotes (A) exhibited strong MDC staining, especially at IC_{50} doses. The same was observed for trypomastigotes (C). The MDC fluorescence intensity is expressed as arbitrary units, where different data represent means ± standard deviation. Fragmented DNA was stained by TUNEL assay and evaluated by flow cytometry; there was insignificant labelling in treated epimastigotes (B) and a remarkable number of labelled trypomastigotes (D). The results were obtained from experiments performed in triplicate.

a few studies have tested the anti-parasitic effects of melittin (Diaz-Achirica *et al*. 1998; Chicharro *et al*. 2001; Luque-Ortega *et al*. 2003; Alberola *et al*. 2004; Pérez-Cordero, 2011) and PLA_2 (Moreira *et al*. 2002; Guillaume *et al*. 2004, Boutrin *et al*. 2008), the two main components of bee venom. Thus far, only 2 studies have shown the lytic effects of melittin on *T. cruzi* epimastigotes and trypomastigotes (Azambuja *et al*. 1989; Fieck *et al*. 2010), and these studies did not investigate the effects on the intracellular forms of the parasites or consider the effects of melittin on host cells. Thus, the aim of this study was to evaluate bee venom as a source of compounds with potential and promising effects for Chagas disease treatment by investigating the *in vitro* effect of *A. mellifera* crude venom on all *T. cruzi* developmental forms, characterizing its target organelles and death phenotypes and evaluating its toxicity to the host cells.

Our results showed that all *T. cruzi* evolutive forms suffered remarkably from the action of the venom. Epimastigotes (i.e., the proliferative insect vector-borne stage), trypomastigotes (i.e., the infective, non-proliferative form), and intracellular amastigotes (i.e., the infective, proliferative form) were found to be sensitive to the venom. The different IC_{50}/1 day or LD_{50}/1 day values indicate that low doses are effective mainly against the infective forms. Additionally, all the *A. mellifera* venom concentrations tested that were effective against the parasite did not exhibit toxicity to the cell host, as observed by TEM and assessed by the Trypan blue exclusion test and the MTS assay.

The electron microscopy analysis of treated parasites strongly suggested that *T. cruzi* parasites were killed by different routes, leading to distinct death phenotypes. This suspicion was reinforced after flow cytometry, fluorimetry and fluorescence microscopy analyses, which revealed distinct staining behaviours in the different parasitic forms.

The cell death process corresponds to the cellular functions lost, originating from morphological, biochemical and/or molecular alterations and occurring through accidental (i.e., passive, with no energy

https://doi.org/10.1017/S0031182012000790 Published online by Cambridge University Press

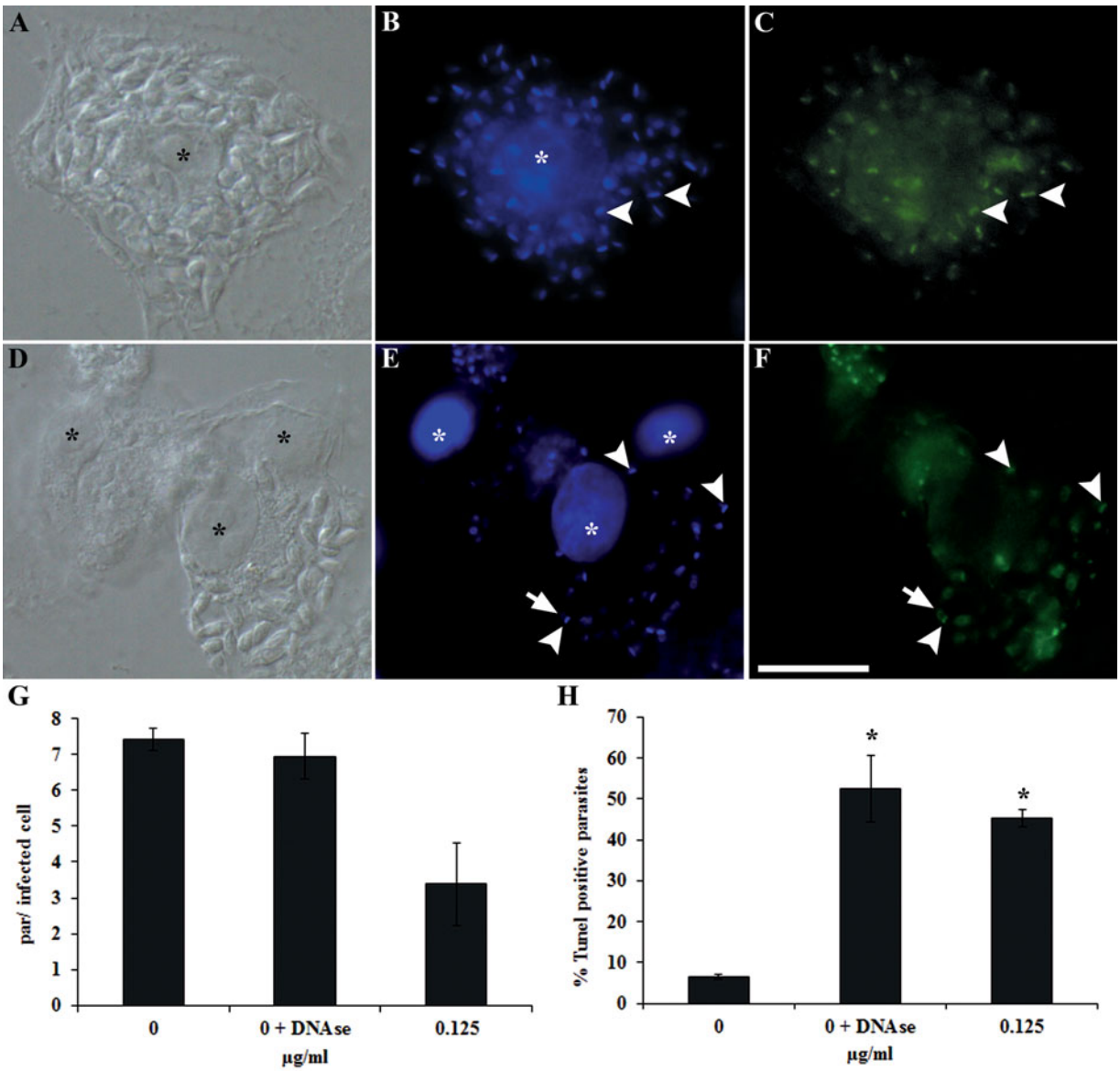

Fig. 7. Fluorescence microscopy of TUNEL labelling in *Trypanosoma cruzi*-infected and venom-treated LLC-MK_2 cells. DAPI (B, E, blue) stained the DNA of the host cell nuclei (asterisks), and kinetoplast (arrowheads) and nuclei (arrows) of intracellular parasites. (A–C) Infected cells incubated with DNAse I, showing a large number of TUNEL-positive parasites (green). (D–F) *Apis mellifera*-treated cells presenting positive staining at nuclei and kinetoplast of intracellular amastigotes (green). (G,H) Inhibition of growth of intracellular amastigotes per infected cell after 3 days of treatment, and the percentage of intracellular parasites positively stained by TUNEL assay. Scale bars: 10 μm.

expenditure) or programmed (i.e., active, with energy outlay) pathways (Sloviter, 2002). Programmed cell death (PCD) is a genetically regulated process and is pivotal to the homeostasis of metazoan organisms, playing a fundamental role in morphogenesis, physiology and host defence against different pathogens, including avoiding an inflammatory response (Guimarães and Linden, 2004). Based on morphological criteria and environmental conditions, PCD has been characterized into different types, such as apoptosis (I-PCD type), autophagy (II-PCD type) and programmed necrosis (III-PCD type) (Kroemer *et al*. 2009). Once triggered, apoptosis is mainly characterized by cytoplasmic retraction; chromatin condensation; chromosomal DNA fragmentation; mitochondrial swelling, with alterations in membrane potential and permeability; exposure of phosphatidylserine residues at the outer plasma membrane; activation of caspases; blebbing of the plasma membrane and the packing of cellular constituents into apoptotic vesicles (Guimarães and Linden, 2004). In contrast, autophagy is a complex signalling pathway involving more than 30 well-conserved Atg proteins that functions to remove and/or remodel damaged cellular structures. It is morphologically characterized by autophagosome formation (i.e., double-membrane vesicles) that is responsible for the engulfment of cytoplasmic constituents, concentric membrane structures in the cytosol and surrounding organelles, and nuclear

https://doi.org/10.1017/S0031182012000790 Published online by Cambridge University Press

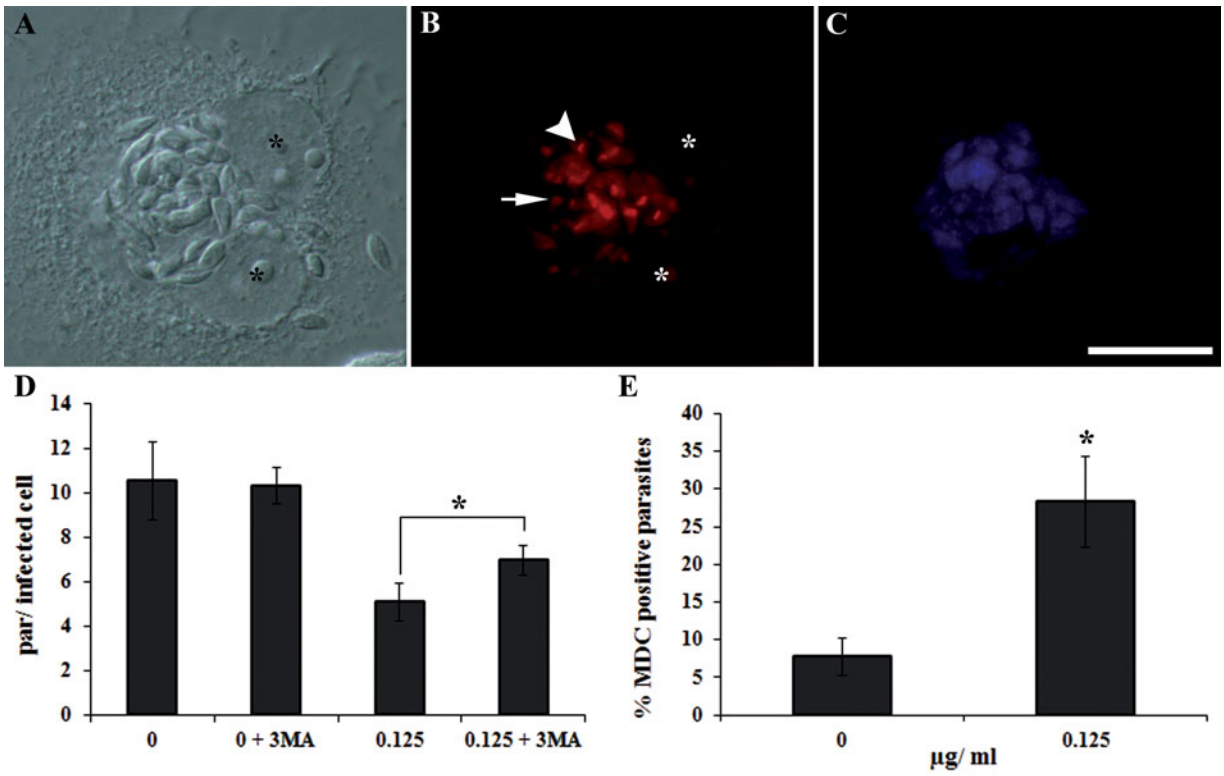

Fig. 8. MDC labelling in *Trypanosoma cruzi*-infected and treated LLC-MK$_2$ cells. (A–C) Fluorescence microscopy where PI (B, red) stained the DNA of the host cell nuclei (asterisks), and the kinetoplast (arrowheads) and nuclei (arrows) of intracellular parasites. (C) Positive staining (blue) exhibited by treated intracellular amastigotes. (D–E) Inhibition of growth of intracellular amastigotes per infected cell after 3 days treatment, in the presence or not of 3-MA, and percentage of intracellular parasites positively stained by MDC assay. The differences between treated parasites in the presence of the inhibitor (D) and treated parasites and non-treated MDC-positive parasites are statistically significant ($P \leqslant 0{\cdot}05$). Scale bars: 10 μm.

limited damage (Tsujimoto and Shimizu, 2005; Meijer *et al*. 2007).

In unicellular eukaryotes, the occurrence and biological relevance of PCD pathways have been strongly demonstrated and debated (Arnoult *et al*. 2001; Debrabant *et al*. 2003; Gordeeva *et al*. 2004). These pathways may play a role in the regulation of parasite number in biological vectors and in definitive host tissues, which can contribute to evasion from host immune defences and in the maintenance of clonality (Lüder *et al*. 2001; Wanderley *et al*. 2006; Kaczanowski *et al*. 2011).

Here, we presented evidence that *A. mellifera* venom-treated parasites exhibited several morphological alterations that are consistent with the main features that characterize autophagy and apoptosis. Treated epimastigotes exhibited strong mitochondrial damage, although their kDNA networks were apparently well preserved. Additionally, the most remarkable feature detected was the endoplasmic reticulum profile surrounding different structures, suggesting autophagosome formation. Some of these alterations were confirmed by the decrease in the mitochondrial potential and the increase in monodansyl cadaverine (MDC) (evaluated by fluorimetry); further, the non-significant percentage of treated epimastigotes labelled by TUNEL staining (a DNA-nicking indicator) reinforced the suggestion of an autophagic cell death phenotype. Morphological changes observed in epimastigotes are in agreement with previous studies that described the capacity of *A. mellifera* venom and its components, such as PLA$_2$ and melittin, to trigger apoptosis (caspase dependent or not) in a great range of tumour cells (Li *et al*. 2006; Chu *et al*. 2007; Wang *et al*. 2009). However, although treated trypomastigotes also exhibited a considerable retraction of the cell body and swollen mitochondria, the most affected structures were the kDNA and the nucleus, which were characterized by profound changes in the filamentous arrays and by chromatin condensation, respectively. Flow cytometry analysis confirmed mitochondrial membrane depolarization but, unlike epimastigotes, treated trypomastigotes exhibited an increased number of cells that tested positive for TUNEL staining and low MDC fluorescence emission, strongly suggesting an apoptosis-like death phenotype. The analyses at the electron microscope of venom-treated intracellular amastigotes did not indicate any preferential kind of cellular phenotype death. The investigation with TUNEL reaction, MDC staining and 3-MA inhibitor, indicated that the treatment induced different cell

https://doi.org/10.1017/S0031182012000790 Published online by Cambridge University Press

death types, although apoptosis has been the most frequently observed (I-PDC type, up to 47·5% TUNEL-positive), followed by the autophagy (II-PDC type, up to 36% MDC-positive). Probably, the remaining 16·5% occurs by another cell death phenotype, such as necrosis (III-PCD type), that was not investigated in the present study. Additionally, taking into account the percentage of PI-positive cells after *A. mellifera* treatment, we can not disregard the fact that some of the treated epimastigotes and trypomastigotes were probably dying by necrosis. However, considering the ultrastructural observations and the use of different PCD probes analysed by fluorescence microscopy, fluorimetry and flow cytometry, treatment with the venom seemed to preferentially generate autophagy- and apoptosis-like cell death in epimastigotes and trypomastigotes, respectively.

Apoptosis-like cell death has already been reported in trypanosomatids, which have complex life cycles that involve multiple hosts, and its occurrence could influence their destiny, favouring their survival in their digenetic life cycle (Nguewa *et al*. 2004; Duszenko *et al*. 2006; Wanderley *et al*. 2009). Furthermore, many anti-parasitic agents have been reported to induce apoptotic-like death in trypanosomatids (Lee *et al*. 2002; De Souza *et al*. 2006; Menna-Barreto *et al*. 2009*a*,*b*), including animal venom such as *Bothrops jararaca* snake venom and its purified L-amino acid oxidase, in treated *T. cruzi* epimastigotes (Deolindo *et al*. 2005, 2010). This treatment caused mitochondrial swelling with an associated loss of membrane potential, kinetoplast disorganization, phosphatidylserine exposure, cytoplasmic retraction and DNA fragmentation (as determined by TUNEL staining). All these features are very similar to those of the *T. cruzi* trypomastigotes incubated with *A. mellifera* venom presented here, in addition to nuclear envelope dilatation and increased nuclear chromatin condensation, which was observed in bloodstream trypomastigotes treated with aromatic diamidines (De Souza *et al*. 2006).

In a similar manner, autophagy has been described in different protozoans, including all pathogenic trypanosomatids (Kiel, 2010; Duszenko *et al*. 2011). Because these parasites display different metabolic profiles depending on their life-cycle stage, autophagy is crucial for organelle turnover, maintaining the metabolic balance and recycling of cellular structures during normal cell growth, and its deregulation or over-stimulus leads to cell death without an inflammatory response (Besteiro *et al*. 2006; Alvarez *et al*. 2008). Different compounds have shown the capacity to induce trypanosomatid death by autophagy (Bera *et al*. 2003; Delgado *et al*. 2009; Schurigt, *et al*. 2010; Sandes *et al*. 2010; Monte Neto *et al*. 2011), with the interesting finding that some drugs can promote different PCD pathways (including autophagy) in distinct morphological parasite forms, such as exhibited by naphthoimidazoles over *T. cruzi* epimastigotes and trypomastigotes (Menna-Barreto *et al*. 2009*a*). Our results followed this pattern. In contrast to trypomastigotes, treatment of *T. cruzi* epimastigotes with the bee venom resulted in remarkable evidence of autophagy-like death. Other reports relate the occurrence of different PCD phenotypes caused by treatment with the same compound in *Leishmania* sp. (Monte-Neto *et al*. 2010; Schurigt *et al*. 2010) and *T. cruzi* (Menna-Barreto *et al*. 2009*b*; Sandes *et al*. 2010).

Some evidence has demonstrated that there is cross-talk and convergence between all PCD pathways in mammalian cells (Guimarães and Linden, 2004). Because the different kinds of cellular death are controlled by signalling networks that frequently overlap, one stimulus can trigger apoptosis and autophagy in the same cell (Golstein and Kroemer, 2005; Levine and Yuan, 2005). Many model systems support the model that different cell death programmes may be triggered in distinct circumstances, such that an apoptotic death morphology can be produced without the involvement of caspases and that autophagic execution pathways may be engaged without either the involvement of caspases or morphological signs of apoptosis (Guimarães and Linden, 2004). Each death phenotype can be variably expressed in different eukaryotic species and among distinct cell types within the same species and can be induced in a context-dependent fashion by identical initiating stimuli (Golstein and Kroemer, 2005). Our results can be considered in this context, in which *A. mellifera* venom treatment generated distinct cell death profiles in *T. cruzi*.

CONCLUSIONS

Chagas disease is an important neglected disease for which there is still inefficient chemotherapy and no vaccine. Furthermore, critical challenges remain, such as vectorial and oral transmission. The recent discovery of PCD occurrence in protozoan parasites encourages the investigation into the ideal drug for the treatment of chagasic patients, which must be capable of killing the *T. cruzi* parasite without triggering host defences. Natural products, such as *A. mellifera* bee venom, are available in different ecosystems around the world and are a great source for compound investigation and drug development. Our findings demonstrate that all *T. cruzi* developmental forms were acted upon by *A. mellifera* venom and displayed different PCD phenotypes. Thus, the regulation and modulation of these cell death routes requires more research to facilitate the development of specific and controlled therapeutic agents. These results are in agreement with previously published data that highlighted the potential use of animal venom as a tool for new therapeutic approaches.

https://doi.org/10.1017/S0031182012000790 Published online by Cambridge University Press

ACKNOWLEDGEMENTS

We thank Edna Lúcia dos Santos Rocha, Lusinete da Rocha Bonfim and Tarcísio Corrêa for valuable technical assistance. This work was supported by Conselho Nacional de Desenvolvimento Científico e Tecnológico (CNPq- 302440/2008–9 and Universal- 476564/ 2010–7) and Fundação de Amparo a Pesquisa do Estado do Rio de Janeiro (FAPERJ- E-26/ 102·581/2010, Pensa Rio- E-26/ 110·313/2010, Pronex- E-26/110·576/2010 and Cientista do Nosso Estado- E-26/102·299/2009).

REFERENCES

Adade, C. M., Cons, B. L., Melo, P. A. and Souto-Padrón, T. (2011). Effect of *Crotalus viridis viridis* snake venom on the ultrastructure and intracellular survival of *Trypanosoma cruzi*. *Parasitology* **138**, 46–58. doi: 10.1017/S0031182010000958.

Alberola, J., Rodríguez, A., Francino, O., Roura, X., Rivas, L. and Andreu, D. (2004). Safety and efficacy of antimicrobial peptides against naturally acquired leishmaniasis. *Antimicrobial Agents and Chemotherapy* **48**, 641–643. doi: 10.1128/AAC.48.2.641–643.2004.

Altmann, K. H. (2001). Microtubule-stabilizing agents: a growing class of important anticancer drugs. *Current Opinion in Chemical Biology* **5**, 424–431. doi: 10.1016/S1367-5931(00)00225-8.

Alvarez, V. E., Kosec, G., Sant Anna, C., Turk, V., Cazzulo, J. J., Turk, B. (2008). Blocking autophagy to prevent parasite differentiation: a possible new strategy for fighting parasitic infections? *Autophagy*. **4**, 361–363. doi: 10.1074/jbc.M708474200.

Arnoult, D., Tatischeff, I., Estaquier, J., Girard, M., Sureau, F., Tissier, J. P., Grodet, A., Dellinger, M., Traincard, F., Kahn, A., Ameisen, J. C. and Petit, P. X. (2001). On the evolutionary conservation of the cell death pathway: mitochondrial release of an apoptosis-inducing factor during *Dictyostelium discoideum* cell death. *Molecular Biology of the Cell* **12**, 3016–3030.

Azambuja, P., Mello, C. B., D'Escoffier, L. N. and Garcia, E. S. (1989). *In vitro* cytotoxicity of *Rhodnius prolixus* hemolytic factor and melittin towards different trypanosomatids. *Brazilian Journal of Medical and Biological Research* **22**, 597–599.

Bechinger, B. (1997). Structure and functions of channel-forming peptides: magainins, cecropins, melittin and alamethicin. *The Journal of Membrane Biology* **156**, 197–211. doi: 10.1007/s002329900201.

Bera, A., Singh, S., Nagaraj, R. and Vaidya, T. (2003). Induction of autophagic cell death in *Leishmania donovani* by antimicrobial peptides. *Molecular and Biochemical Parasitology* **127**, 23–35. doi: 10.1016/S0166-685 (02)00300-6.

Berridge, M. V., Herst, P. M. and Tan, A. S. (2005). Tetrazolium dyes as tools in cell biology: new insights into their cellular reduction. *Biotechnology Annual Review* **11**, 127–152. doi: 10.1016/S1387-2656(05)11004-7.

Besteiro, S., Williams, R. A., Morrison, L. S., Coombs, G. H. and Mottram, J. C. (2006). Endosome sorting and autophagy are essential for differentiation and virulence of *Leishmania major*. *The Journal of Biological Chemistry* **281**, 11384–11396. doi: 10.1074/jbc.M512307200.

Blondelle, S.E. and Houghten, R. A. (1991). Hemolytic and antimicrobial activities of twenty-four individual omission analogues of melittin. *Biochemistry* **30**, 4671–4678. doi: 10.1021/bi00233a006.

Boutrin, M.-C. F., Foster, H. A. and Pentreath, V. W. (2008). The effects of bee (*Apis mellifera*) venom phospholipase A2 on *Trypanosoma brucei brucei* and enterobacteria. *Experimental Parasitology* **119**, 246–251. doi: 10.1016/j.exppara.2008.02.002.

Brand, G. D., Leite, J. R., De Sa Mandel, S. M., Mesquita, D. A., Silva, L. P., Prates, M. V., Barbosa, E. A., Vinecky, F., Martins, G. R., Galasso, J. H., Kuchelhaus, S. A., Sampaio, R. N., Furtado, J. R., Andrade, A. C. and Bloch, C. (2006). Novel dermaseptins from *Phyllomedusa hypochondrialis* (Amphibia). *Biochemical and Biophysical Research Communications* **347**, 739–746. doi: 10.1016/j.bbrc.2006.06.168.

Chen, Y. N., Li, K. C., Li, Z., Shang, G. W., Liu, D. N., Lu, Z. M., Zhang, J. W., Ji, Y. H., Gao, G. D. and Chen, J. (2006). Effects of bee venom peptidergic components on rat pain-related behaviors and inflammation. *Neuroscience* **138**, 631–640. doi: 10.1016/j.neuroscience.2005.11.022.

Chicharro, C., Granata, C., Lozano, R., Andreu, D. and Rivas, L. (2001). N-terminal fatty acid substitution increases the leishmanicidal activity of CA(1–7)M(2–9), a cecropin-melittin hybrid peptide. *Antimicrobial Agents and Chemotherapy* **45**, 2441–2449. doi: 10.1128/AAC.45.9.2441-2449.2001.

Chu, S. T., Cheng, H. H., Huang, C. J., Chang, H. C., Chi, C. C., Su, H. H., Hsu, S. S., Wang, J. L., Chen, I. S., Liu, S. I., Lu, Y. C., Huang, J. K., Ho, C. M. and Jan, C. R. (2007). Phospholipase A2-independent Ca2 + entry and subsequent apoptosis induced by melittin in human MG63 osteosarcoma cells. *Life Sciences* **80**, 364–369. doi: 10.1016/j.lfs.2006.09.024.

Ciscotto, P., Machado de Avila, R. A., Coelho, E. A. F., Oliveira, J., Diniz, C. G., Farías, L. M., Carvalho, M. A. R., Maria, W. S., Sanchez, E. F., Borges, A. and Chávez-Olórtegui, C. (2009). Antigenic, microbicidal and antiparasitic properties of an L -amino acid oxidase isolated from *Bothrops jararaca* snake venom. *Toxicon* **53**, 330–341. doi: 10.1016/j.toxicon.2008.12.004.

De Souza, E. M., Menna-Barreto, R., Araújo-Jorge, T. C., Kumar, A., Hu, Q., Boykin, D. W. and Soeiro, M. N. (2006). Antiparasitic activity of aromatic diamidines is related to apoptosis-like death in *Trypanosoma cruzi*. *Parasitology* **133**, 75–79. doi: 10.1017/S0031182006000084.

Debrabant, A. and Nakhasi, H. (2003). Programmed cell death in trypanosomatids: is it an altruistic mechanism for survival of the fittest? *Kinetoplastid Biology and Disease* **2**, 7. doi: 10.1186/1475-9292-2-7.

Delgado, M., Anderson, P., Garcia-Salcedo, J. A., Caro, M. and Gonzalez-Rey, E. (2009). Neuropeptides kill African trypanosomes by targeting intracellular compartments and inducing autophagic-like cell death. *Cell Death and Differentiation* **16**, 406–416. doi: 10.1038/cdd.2008.161.

Deolindo, P., Teixeira-Ferreira, A. S., DaMatta, R. A. and Alves, E. W. (2010). L-amino acid oxidase activity present in fractions of *Bothrops jararaca* venom is responsible for the induction of programmed cell death in *Trypanosoma cruzi*. *Toxicon* **56**, 944–955. doi: 10.1016/j.toxicon.2010.06.019.

Deolindo, P., Teixeira-Ferreira, A. S., Melo, E. J. T., Arnholdt, A. C. V., De Souza, W., Alves, E. W. and DaMatta, R. A. (2005). Programmed cell death in *Trypanosoma cruzi* induced by *Bothrops jararaca* venom. *Memórias do Instituto Oswaldo Cruz* **100**, 33–38. doi: 10.1590/S0074-02762005000100006.

Díaz-Achirica, P., Ubach, J., Guinea, A., Andreu, D. and Rivas, L. (1998). The plasma membrane of *Leishmania donovani* promastigotes is the main target for CA(1–8)M(1–18), a synthetic cecropin A-melittin hybrid peptide. *The Biochemical Journal* **330**, 453–460.

Duszenko, M., Figarella, K., Macleod, E. T. and Welburn, S. C. (2006). Death of a trypanosome: a selfish altruism. *Trends in Parasitology* **22**, 536–542. doi: 10.1016/j.pt.2006.08.010.

Duszenko, M., Ginger, M. L., Brennand, A., Gualdrón-López, M., Colombo, M. I., Coombs, G. H., Coppens, I., Jayabalasingham, B., Langsley, G., De Castro, S. L., Menna-Barreto, R., Mottram, J. C., Navarro, M., Rigden, D. J., Romano, P. S., Stoka, V., Turk, B. and Michels, P. A. (2011). Autophagy in protists. *Autophagy* **7**, 127–158. doi: 10.4161/auto.7.2.13310.

Fernandez-Gomez, R., Zerrouk, H., Sebti, F., Loyens, M., Benslimane, A. and Ouaissi, M. A. (1994). Growth inhibition of *Trypanosoma cruzi* and *Leishmania donovani* infantum by different snake venoms: Preliminary identification of proteins from *Cerastes cerastes* venom wich interact with the parasites. *Toxicon* **32**, 875–882. doi: 10.1016/ 0041-0101(94)90366-2.

Fieck, A., Hurwitz, I., Kang, A. S. and Durvasula, R. (2010). *Trypanosoma cruzi*: synergistic cytotoxicity of multiple amphipathic antimicrobial peptides to T. cruzi and potential bacterial hosts. *Experimental Parasitology* **125**, 342–347. doi: 10.1016/j.exppara.2010.02.016.

Fox, J. W. and Serrano, S. M. (2007). Approaching the golden age of natural product pharmaceuticals from venom libraries: an overview of toxins and toxin-derivatives currently involved in therapeutic or diagnostic applications. *Current Pharmaceutical Design* **13**, 2927–2934.

Golstein, P. and Kroemer, G. (2005). Redundant cell death mechanisms as relics and backups. *Cell Death and Differentiation* **12**, 1490–1496. doi: 10.1038/sj.cdd.4401607.

Gonçalves, A. R., Soares, M. J., De Souza, W., DaMatta, R. A. and Alves, E. W. (2002). Ultrastructural alterations and growth inhibition of *Trypanosoma cruzi* and *Leishmania major* induced by *Bothrops jararaca* venom. *Parasitology Research* **88**, 598–602. doi: 10.1007/s00436-002-0626-3.

Gordeeva, A. V., Labas, Y. A. and Zvyagilskaya, R. A. (2004). Apoptosis in unicellular organisms: mechanisms and evolution. *Biochemistry* **69**, 1055–1066. doi: 10.1023/B:BIRY.0000046879.54211.ab.

Guillaume, C., Deregnaucourt, C., Clavey, V. and Schrével, J. (2004). Anti-Plasmodium properties of group IA, IB, IIA and III secreted phospholipases A2 are serum-dependent. *Toxicon* **43**, 311–318. doi: 10.1016/j.toxicon.2004.01.006.

Guimarães, C. A. and Linden, R. (2004). Programmed cell deaths. *Apoptosis and alternative deathstyles*. European Journal of Biochemistry **271**, 1638–1650. doi: 10.1111/j.1432-1033.2004.04084.x.

Habermann, E. (1972). Bee and wasp venoms. *Science* **177**, 314–322.

Holle, L., Song, W., Holle, E., Wei, Y., Li, J., Wagner, T. E. and Yu, X. (2009). In vitro- and in vivo-targeted tumor lysis by an MMP2 cleavable melittin-LAP fusion protein. *International Journal of Oncology* **35**, 829–835. doi: 10.3892/ijo_00000396.

Huh, J. E., Baek, Y. H., Lee, M. H., Choi, D. Y., Park, D. S. and Lee, J. D. (2010). Bee venom inhibits tumor angiogenesis and metastasis by inhibiting tyrosine phosphorylation of VEGFR-2 in LLC-tumor-bearing mice. *Cancer Letters* **292**, 98–110. doi: 10.1016/j.canlet.2009.11.013.

Kaczanowski, S., Sajid, M. and Reece, S.E. (2011). Evolution of apoptosis-like programmed cell death in unicellular protozoan parasites. *Parasites & Vectors* **4**, 44. doi: 10.1186/1756-3305-4-44.

Kiel, J. A. (2010). Autophagy in unicellular eukaryotes. *Philosophical Transactions of the Royal Society of London, Series B i* **365**, 819–830. doi: 10.1098/rstb.2009.0237.

Kirkpatrick, P. (2002). Antibacterial drugs: stitching together naturally. *Nature Reviews Drug Discovery* **1**, 748. doi: 10.1038/nrd921.

Kroemer, G., Galluzzi, L., Vandenabeele, P., Abrams, J., Alnemri, E. S., Baehrecke, E. H., Blagosklonny, M. V., El-Deiry, W. S., Golstein, P., Green, D. R., Hengartner, M., Knight, R. A., Kumar, S., Lipton, S. A., Malorni, W., Nuñez, G., Peter, M. E., Tschopp, J., Yuan, J., Piacentini, M., Zhivotovsky, B. and Melino, G. (2009). Classification of cell death: recommendations of the Nomenclature Committee on Cell Death 2009. *Cell Death and Differentiation* **16**, 3–11. doi: 10.1038/cdd.2008.150.

Kwon, Y. B., Lee, H. J., Han, H. J., Mar, W. C., Kang, S. K., Yoon, O. B., Beitz, A. J. and Lee, J. H. (2002). The water-soluble fraction of bee venom produces antinociceptive and anti-inflammatory effects on rheumatoid arthritis in rats. *Life Sciences* **71**, 191–204. doi: 10.1016/S0024-3205(02)01617-X.

Lee, N., Bertholet, S., Debrabant, A., Muller, J., Duncan, R. and Nakhasi, H. L. (2002). Programmed cell death in the unicellular protozoan parasite *Leishmania*. *Cell Death and Differentiation* **9**, 53–64. doi: 10.1038/sj/cdd/4400952.

Levine, B. and Yuan, J. (2005). Autophagy in cell death: an innocent convict? *The Journal of Clinical Investigation* **115**, 2679–2688. doi: 10.1172/JCI26390.

Lewis, R. J. and Garcia, M. L. (2003). Therapeutic potential of venom peptides. *Nature Reviews Drug Discovery* **2**,790–802. doi: 10.1038/nrd1197.

Li, B., Gu, W., Zhang, C., Huang, X. Q., Han, K. Q. and Ling, C. Q. (2006). Growth arrest and apoptosis of the human hepatocellular carcinoma cell line BEL-7402 induced by melittin. *Onkologie* **29**, 367–371. doi: 10.1159/000094711.

Lüder, C. G., Gross, U. and Lopes, M. F. (2001). Intracellular protozoan parasites and apoptosis: diverse strategies to modulate parasite-host interactions. *Trends in Parasitology* **17**, 480–486. doi: 10.1016/S1471-4922(01)02016-5.

Luque-Ortega, J. R., Saugar, J. M., Chiva, C., Andreu, D. and Rivas, L. (2003). Identification of new leishmanicidal peptide lead structures by automated real-time monitoring of changes in intracellular ATP. *The Biochemical Journal* **375**, 221–230. doi: 10.1042/BJ20030544.

Meijer, W. H., van der Klei, I. J., Veenhuis, M. and Kiel, J. A. (2007). ATG genes involved in non-selective autophagy are conserved from yeast to man, but the selective Cvt and pexophagy pathways also require organism-specific genes. *Autophagy* **3**, 106–116.

Menna-Barreto, R. F. S., Corrêa, J. R., Cascabulho, C. M., Fernandes, M. C., Pinto, A. V., Soares, M. J. and De Castro, S. L. (2009*a*). Naphthoimidazoles promote different death phenotypes in *Trypanosoma cruzi*. *Parasitology* **136**, 499–510. doi: 10.1017/S0031182009005745.

Menna-Barreto, R. F. S., Salomão, K., Dantas, A. P., Santa-Rita, R. M., Soares, M. J., Barbosa, H. S. and De Castro, S. L. (2009*b*). Different cell death pathways induced by drugs in *Trypanosoma cruzi*: An ultrastructural study. *Micron* **40**, 157–168. doi: 10.1016/j.micron.2008.08.003.

Moncayo, A. and Silveira, A. C. (2009). Current epidemiological trends for Chagas disease in LatinAmerica and future challenges in epidemiology, surveillance and health policy. *Memórias do Instituto Oswaldo Cruz* **104**, 17–30. doi: 10.1590/S0074-02762009000900005.

Monte Neto, R. L., Sousa, L. M., Dias, C. S., Barbosa Filho, J. M., Oliveira, M. R. and Figueiredo, R. C. (2011). Morphological and physiological changes in *Leishmania* promastigotes induced by yangambin, a lignan obtained from *Ocotea duckei*. *Experimental Parasitology* **127**, 215–221. doi: 10.1016/j.exppara.2010.07.020.

Moreira, L. A., Ito, J., Ghosh, A., Devenport, M., Zieler, H., Abraham, E. G., Crisanti, A., Nolan, T., Catteruccia, F. and Jacobs-Lorena, M. (2002). Bee venom phospholipase inhibits malaria parasite development in transgenic mosquitoes. *The Journal of Biological Chemistry* **277**, 40839–40843. doi: 10.1074/jbc.M206647200.

Nguewa, P. A., Fuertes, M. A., Valladares, B., Alonso, C. and Pérez, J. M. (2004). Programmed cell death in trypanosomatids: a way to maximize their biological fitness? *Trends in Parasitology* **20**, 375–380. doi: 10.1016/j.pt.2004.05.006.

Papo, N. and Shai, Y. (2003). Can we predict biological activity of antimicrobial peptides from their interactions with model phospholipid membranes? *Peptides* **24**, 1693–1703. doi: 10.1016/j.peptides.2003.09.013.

Park, H. J., Lee, S. H., Son, D. J., Oh, K. W., Kim, K. H., Song, H. S., Kim, G. J., Oh, G. T., Yoon, D. Y. and Hong, J. T. (2004). Antiarthritic effect of bee venom: inhibition of inflammation mediator generation by suppression of NF-kappaB through interaction with the p50 subunit. *Arthritis and Rheumatism* **50**, 3504–3515. doi: 10.1002/art.20626.

Park, M. H., Choi, M. S., Kwak, D. H., Oh, K. W., Yoon do, Y., Han, S. B., Song, H. S., Song, M. J. and Hong, J. T. (2011). Anti-cancer effect of bee venom in prostate cancer cells through activation of caspase pathway via inactivation of NF-κB. *Prostate* **71**, 801–812. doi: 10.1002/pros.21296.

Passero, L. F. D., Tomokane, T. Y., Corbett, C. E. P., Laurenti, M. D. and Toyama, M. H. (2007). Comparative studies of the anti-leishmanial activity of three *Crotalus durissus* ssp. *venoms*. Parasitology Research **101**, 1365–1371. doi: 10.1007/s00436-007-0653-1.

Pérez-Cordero, J. J., Lozano, J. M., Cortés, J. and Delgado, G. (2011). Leishmanicidal activity of synthetic antimicrobial peptides in an infection model with human dendritic cells. *Peptides* **32**, 683–690. doi: 10.1016/j.peptides.2011.01.011.

Putz, T., Ramoner, R., Gander, H., Rahm, A., Bartsch, G., Bernardo, K., Ramsay, S. and Thurnher, M. (2007). Bee venom secretory phospholipase A2 and phosphatidylinositol-homologues cooperatively disrupt membrane integrity, abrogate signal transduction and inhibit proliferation of renal cancer cells. *Cancer Immunology and Immunotherapy* **56**, 627–640. doi: 10.1007/s00262-006-0220-0.

Putz, T., Ramoner, R., Gander, H., Rahm, A., Bartsch, G. and Thurnher, M. (2006). Antitumor action and immune activation through cooperation of bee venom secretory phospholipase A2 and phosphatidylinositol-(3,4)-bisphosphate. *Cancer Immunology and Immunotherapy* **55**, 1374–1383. Doi: 10.1007/s00262-006-0143-9.

Raghuraman, H. and Chattopadhyay, A. (2007). Melittin: a membrane-active peptide with diverse functions. *Bioscience Reports* **27**, 189–223. doi: 10.1007/s10540-006-9030-z.

Rassi Jr, A., Rassi, A. and Marin-Neto, J. A. (2009). Chagas heart disease: pathophysiologic mechanisms, prognostic factors and risk stratification. *Memórias do Instituto Oswaldo Cruz* **104**, 152–158. doi: 10.1590/S0074-02762009000900021.

Sandes, J. M., Borges, A. R., Junior, C. G., Silva, F. P., Carvalho, G. A., Rocha, G. B., Vasconcellos, M. L. and Figueiredo, R. C. (2010). 3-Hydroxy-2-methylene-3-(4-nitrophenylpropanenitrile): A new highly active compound against epimastigote and trypomastigote form of *Trypanosoma cruzi*. *Bioorganic Chemistry* **38**, 190–195. doi: 10.1016/j.bioorg.2010.06.003.

Schurigt, U., Schad, C., Glowa, C., Baum, U., Thomale, K., Schnitzer, J. K., Schultheis, M., Schaschke, N., Schirmeister, T. and Moll, H. (2010). Aziridine-2,3-dicarboxylate-based cysteine cathepsin inhibitors induce cell death in *Leishmania major* associated with accumulation of debris in autophagy-related lysosome-like vacuoles. *Antimicrobial Agents and Chemotherapy* **54**, 5028–5041. doi: 10.1128/AAC.00327-10.

Sloviter, R. S. (2002). Apoptosis: a guide for the perplexed. *Trends in Pharmacological Sciences* **23**, 19–24. doi: 10.1016/S0165-6147(00)01867-8.

Son, D. J., Lee, J. W., Lee, Y. H., Song, H. S., Lee, C. K. and Hong, J. T. (2007). Therapeutic application of anti-arthritis, pain-releasing, and anti-cancer effects of bee venom and its constituent compounds. *Pharmacology & Therapeutics* **115**, 246–270. doi: 10.1016/j.pharmthera.2007.04.004.

Tempone, A. G., Andrade, H. F., Spencer, P. J., Lourenço, C. O., Rogero, J. R. and Nascimento, N. (2001). Bothrops moojeni venom kills *Leishmania* spp. with hydrogen peroxide generated by its L-amino acid oxidase. *Biochemical and Biophysical Research Communications* **280**, 620–624. doi: 10.1006/bbrc.2000.4175.

Tempone, A. G., Sartorelli, P., Mady, C. and Fernandes, F. (2007). Natural products to anti-trypanosomal drugs: an overview of new drug prototypes for American Trypanosomiasis. *Cardiovascular & Hematological Agents in Medicinal Chemistry* **5**, 222–235. doi: 10.2174/187152507781058726.

Toyama, M. H., Toyama, D. O., Passero, L. F., Laurenti, M. D., Corbett, C. E., Tomokane, T. Y., Fonseca, F. V., Antunes, E., Joazeiro, P. P., Beriam, L. O., Martins, M. A., Monteiro, H. S. and Fonteles, M. C. (2006). Isolation of a new L-amino acid oxidase from

Crotalus durissus cascavella venom. *Toxicon* **47**, 47–57. doi: 10.1016/j.toxicon.2005.09.008.

Tsujimoto, Y. and Shimizu, S. (2005). Another way to die: autophagic programmed cell death. *Cell Death and Differentiation* **12**, 1528–1534. doi: 10.1038/sj.cdd.4401777.

Urbina, J. A. and Docampo, R. (2003). Specific chemotherapy of Chagas disease: controversies and advances. *Trends in Parasitology* **19**, 495–501. doi: 10.1016/j.pt.2003.09.001.

Wanderley, J. L., Moreira, M. E., Benjamin, A., Bonomo, A. C. and Barcinski, M. A. (2006). Mimicry of apoptotic cells by exposing phosphatidylserine participates in the establishment of amastigotes of *Leishmania* (*L*) *amazonensis* in mammalian hosts. *Journal of Immunology* **176**, 1834–1839.

Wanderley, J. L., Pinto da Silva, L. H., Deolindo, P., Soong, L., Borges, V. M., Prates, D. B., de Souza, A. P., Barral, A., Balanco, J. M., do Nascimento, M. T., Saraiva, E. M. and Barcinski, M. A. (2009). Cooperation between apoptotic and viable metacyclics enhances the pathogenesis of Leishmaniasis. *PLoS One* **4**, e5733. doi: 10.1371/journal.pone.0005733.

Wang, C., Chen, T., Zhang, N., Yang, M., Li, B., Lü, X., Cao, X. and Ling, C. (2009). Melittin, a major component of bee venom, sensitizes human hepatocellular carcinoma cells to tumor necrosis factor-related apoptosis-inducing ligand (TRAIL)-induced apoptosis by activating CaMKII-TAK1-JNK/p38 and inhibiting IkappaBalpha kinase-NFkappaB. *The Journal of Biological Chemistry* **284**, 3804–3813. doi: 10.1074/jbc.M807191200.

Zieler, H., Keister, D. B., Dvorak, J. A. and Ribeiro, M. C. (2001). A snake venom phospholipase A2 blocks malaria parasite development in the mosquito midgut by inhibiting ookinete association with the midgut surface. *The Journal of Experimental Biology* **204**, 4157–4167.